AWARD NUMBER: W81XWH-14-1-0178

TITLE: Reprogramming of the Ovarian Tumor Stroma by Activation of a Biomechanical ECM Switch

PRINCIPAL INVESTIGATOR: Peter Brooks

CONTRACTING ORGANIZATION: Maine Medical Center
Portland, ME 04102

REPORT DATE: July 2015

TYPE OF REPORT: Annual

PREPARED FOR: U.S. Army Medical Research and Materiel Command
Fort Detrick, Maryland 21702-5012

DISTRIBUTION STATEMENT: Approved for Public Release;
Distribution Unlimited

REPORT DOCUMENTATION PAGE

Form Approved
OMB No. 0704-0188

1. REPORT DATE
July 2015

2. REPORT TYPE
Annual

3. DATES COVERED
7/15-14-7/14/15

4. TITLE AND SUBTITLE

Reprogramming of the Ovarian Tumor Stroma by Activation of a Biomechanical ECM Switch

5a. CONTRACT NUMBER
W81XWH-14-1-0178

5b. GRANT NUMBER

5c. PROGRAM ELEMENT NUMBER

6. AUTHOR(S)

Peter Brooks, PhD

E-Mail: brookp1@mmc.org

5d. PROJECT NUMBER

5e. TASK NUMBER

5f. WORK UNIT NUMBER

7. PERFORMING ORGANIZATION NAME(S) AND ADDRESS(ES)

Maine Medical Center
22 Bramhall Street
Portland, ME 04102-3134

8. PERFORMING ORGANIZATION REPORT NUMBER

9. SPONSORING / MONITORING AGENCY NAME(S) AND ADDRESS(ES)

U.S. Army Medical Research and Materiel Command
Fort Detrick, Maryland 21702-5012

10. SPONSOR/MONITOR'S ACRONYM(S)

11. SPONSOR/MONITOR'S REPORT NUMBER(S)

12. DISTRIBUTION / AVAILABILITY STATEMENT

Approved for Public Release; Distribution Unlimited

13. SUPPLEMENTARY NOTES

14. ABSTRACT

Ovarian cancer is among the most lethal forms of gynecological malignancies with limited durable responses observed following front line treatment for late stage recurrent disease. We have proposed to assess the role of α10β1 on tumor growth and chemosensitivity in vivo. We have made significant progress towards the completion of the overall goals of this project during this initial funding period. In particular, we, have characterized stromal cell infiltration of ovarian tumors and have shown extensive infiltration of tumor associated blood vessels as well as fibroblasts which can express high levels of pro-tumorigenic cytokines. Targeting the HU177 collagen epitope recognized by a α10β1 significantly reduced angiogenesis and fibroblast infiltration. Interestingly, while reducing expression of α10β1 can inhibit fibroblast migration on denatured collagen, it failed to reduce cell adhesion. Moreover a peptide antagonist of α10β1 may inhibit ovarian tumor growth in vivo. Finally, our studies suggest that the number and size of ovarian tumors was reduced in transgenic mice that lack α10β1 and a reduction in stromal cell infiltration was observed in tumors from α10β1 null mice. Collectively, our new findings support the hypothesis that α10β1 plays a role in regulating stromal cell behavior and ovarian tumor growth.

15. SUBJECT TERMS

Ovarian cancer αSMA Integrin α10β1 Stromal Fibroblast Angiogenesis Cisplatin Chemosensitivity Cell adhesion Cell migration Cell proliferation Cytokines

16. SECURITY CLASSIFICATION OF:			**17. LIMITATION OF ABSTRACT**	**18. NUMBER OF PAGES**	**19a. NAME OF RESPONSIBLE PERSON**
a. REPORT	**b. ABSTRACT**	**c. THIS PAGE**			USAMRMC
Unclassified	Unclassified	Unclassified	Unclassified	53	**19b. TELEPHONE NUMBER** *(include area code)*

Table of Contents

Page

1). Introduction: Ovarian cancer is among the most lethal forms of gynecological malignancies with limited durable responses observed following front line treatment for late stage recurrent disease. The limited impact of chemotherapy and specific targeted agents on recurrent ovarian carcinoma implies the involvement of previously unknown signaling mechanisms, as well as the potential influence of altered stromal components. However, little is known concerning how these stromal cells are reprogrammed to promote ovarian tumor growth or regulate chemosensitivity. Accumulating evidence from both biochemical experiments and biophysical studies have demonstrated extensive collagen remodeling in ovarian tumor as compared to normal tissues. This differential ECM configuration might provide a unique means for selectively regulating stromal cell behavior since interactions with remodeled ECM may alter cell adhesion, migration, proliferation, survival and gene expression. Therefore, the overall goal of this proposal is to test the hypothesis that alterations of the biophysical structure of collagen results in the exposure of a previously unrecognized $\alpha10\beta1$ integrin-binding element that facilitates reprogramming and accumulation of a subset of host derived CAF-like stromal cells that support tumor growth and modulate chemosensitivity. To this end, we have proposed to assess the role of $\alpha10\beta1$ on tumor growth and chemosensitivity in vivo using murine and human ovarian tumor models. We will examine the impact of function blocking antagonists directed to $\alpha10\beta1$ alone and in combination with chemotherapy on ovarian tumor growth in vivo. In addition, we plan identify and characterize cellular and molecular mechanisms by which $\alpha10\beta1$ expressed in the stromal cells modulates tumor growth and chemosensitivity.

2). Key Words:
1). Ovarian cancer
2). αSMA
3). Integrin $\alpha10\beta1$
4). Stromal Fibroblast
5). Angiogenesis
6). Cisplatin
7). Chemosensitivity
8). Cell adhesion
9). Cell migration
10). Cell proliferation
11). Cytokines

<u>3). Accomplishments:</u>
Summary of major goals of project:
A). As outlined in aim 1 (tasks 1-3) we have proposed to analyze the effects of antagonists of $\alpha10\beta1$ alone and in combination with chemotherapy on tumor growth in vivo using both transgenic and wild type human and murine ovarian tumor models. We will carry out a histopathological analysis of the ovarian tumors along with an analysis of potential changes in cytokine expression in both serum and conditioned medium from stromal cells.

B). As outlined in aim 1 (task 4) we have proposed to analyze the growth of ID8 cells mixed with $\alpha10\beta1$ fibroblast variants in mice alone and in combination with chemotherapy. We will carry out a histopathological analysis of the ovarian tumors along with an analysis of changes in cytokine expression in both serum and conditioned medium from stromal cells.

C). As outlined in aim 2 (tasks 1 and 2) we have proposed to analyze the role of $\alpha10\beta1$ in regulating stromal cell adhesion, migration and proliferation on distinct ECM substrates including native and denatured collagen.

D). As outlined in aim 2 (task 3) we have proposed to analyze the role of α10β1 on fibroblast growth factors and cytokines and their impact on ovarian tumor cell behavior.

E). Specific Accomplishments for reporting period as they relate to the major goals described above. We have made significant progress towards the overall goals of our project during this initial funding period (July 2014 through July 2015). Specifically, we have made substantial progress on both specific aims 1 and 2 and their associated tasks. In this regard, studies outlined in this project were used as part of a manuscript that is being submitted for publication (see appendix). A detailed summary of our current the research accomplishments as they pertain to the tasks outlined in the statement of work is provided below.

Characterization of in tumorigenic properties and stromal infiltration of murine ID8 and human SKOV-3 ovarian tumors in in vivo. Our previous studies suggested that targeting the HU177 cryptic epitope recognized by integrin α10β1 inhibited SKOV-3 tumor growth in vivo and reduced the accumulation of αSMA expressing stromal cells by approximately 70%. To further examine changes in stromal infiltration of ovarian tumors as outlined in aim 1, we began first by quantifying basal levels of angiogenesis in SKOV-3 tumors as well as the levels of angiogenesis following treatment with antagonists of the HU177 collagen epitope. As shown in figure 1A and B, mice carrying SKOV-3 tumors exhibited an approximately 35% reduction in angiogenesis as compared to controls. Next we began to establish the working conditions to assess the growth properties of murine ID8 ovarian tumors in C57BL/6 mice. Briefly, ID8 cells ($5x10^6$) were injected subcutaneously into C57BL/6 mice and resulting tumors were analyzed 6 weeks later. As shown in figure 1C, small be definable ID8 ovarian tumors formed as indicated by H&E staining. While solid tumor did form, the resulting tumors were very small and thus a much larger number of tumor cells as well as a longer incubation period will be needed to establish larger tumors for a more accurate analysis. Finally, to assess whether αSMA expressing stromal cells are able to infiltrate these early stage small ID8 tumors, frozen sections were prepared and stained for the presence of αSMA expressing stromal cells. As shown in figure 1D, αSMA expressing stromal cell were readily detected within these ID8 ovarian carcinomas.

A.

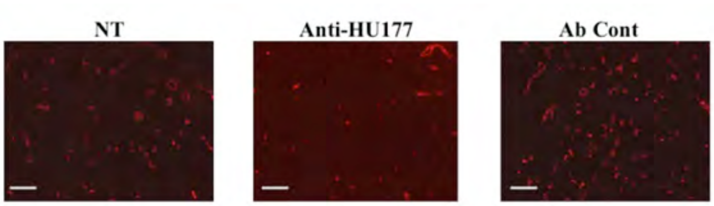

B.

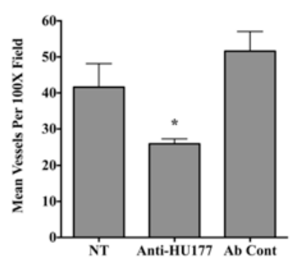

C.

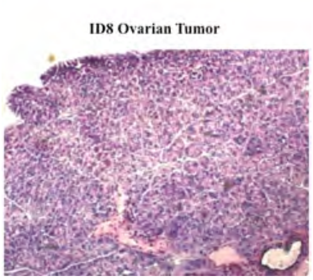

D.

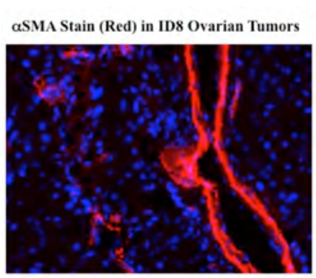

Figure 1. Characterization of in tumorigenic properties and stromal infiltration of murine ID8 and human SKOV-3 ovarian tumors in in vivo. Mice were injected with SKOV-3 cells and untreated or treated with anti-HU177 or control antibodies. A), Examples of tumors from each condition stained for CD-31 (red). B), Quantification of tumor angiogenesis. Data bars represent mean vessels per 100X field ± SE. C), Example of ID8 tumors stained by H&E. D). Example of ID8 tumors stained for expression of αSMA (Red).

Effects of PGF peptide on α10β1 integrin binding to denatured collagen. Our previous studies suggested that integrin α10β1 directly binds the PGF peptide, which contains critical residues within the HU177 cryptic collagen epitope. To examine the ability of the synthetic PGF collagen peptide to act as an antagonist of α10β1 integrin we assessed the ability of the PGF peptide to reduce binding of recombinant α10β1 to denatured collagen in a competition ELISA. As shown in figure 2, incubation of the PGF-peptide, but not a control non-specific peptide with recombinant α10β1 reduced it's binding by approximately 60% as compared with control. These findings are consistent with our previous studies indicating that the Mab directed to the HU177 collagen epitope inhibited α10β1 binding to denatured collagen by approximately 60% and suggest that the PGF-peptide inhibits α10β1 binding at the concentrations tested.

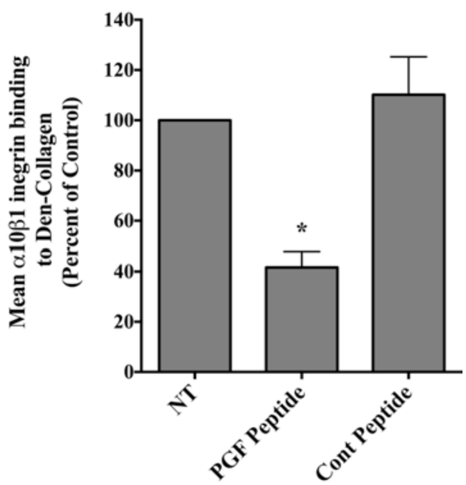

Figure 2. Effects of PGF peptide on α10β1 integrin binding to denatured collagen. Integrin α10β1 binding to denatured collagen in the presence of synthetic HU177 epitope or control peptide. Data bars represent mean integrin binding indicated as percent of control± SE from 3 experiments. * P<0.05 as compared to controls.

Effects of PGF peptide on fibroblast cell adhesion and migration. Given our studies indicating the ability of the PGF peptide to inhibit α10β1-binding activity, we next examined the ability of this peptide to alter fibroblast cell adhesion and migration on denatured collagen. As shown in figure 3A, incubation of αSMA expressing fibroblasts with the PGF collagen peptide resulted in a significant (P<0.05) approximately 50% inhibition of adhesion to denatured collagen. In similar studies the PGF-peptide also significantly (P<0.05) inhibited fibroblast migration by approximately 50% (Figure 3B). Collectively these important findings confirm the function blocking ability of the PGF-peptide to disrupt fibroblast adhesion and migration on denatured collagen.

A.

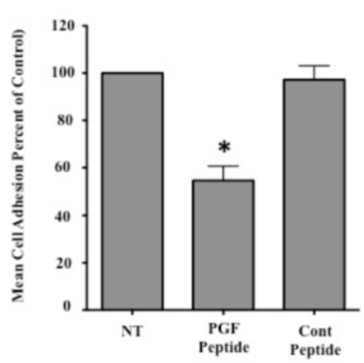

B.

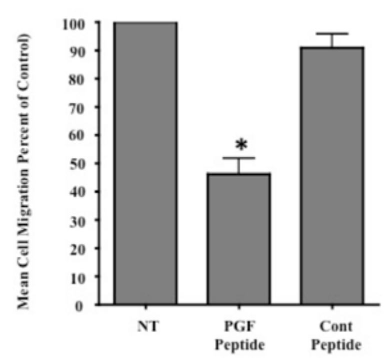

Figure 3. Effects of PGF peptide on fibroblast adhesion and migration on denatured collagen. Human fibroblasts were resuspended in the presence or absence the HU177 cryptic collagen epitope peptide (PGF) or control peptide. A). Data bars represent mean adhesion indicated as percent of control± SE from 3 experiments. B). Data bars represent mean migration indicated as percent of control± SE from 3 experiments. * P<0.05 as compared to controls.

Effects of antagonists of α10β1 alone and in combination with Cisplatin on ovarian tumor growth in vivo. As outlined in specific aim 1, we assess the effects of combining Cisplatin with antagonists of the α10β1. Nude mice were first injected with SKOV-3 human ovarian tumor cells and 3 days later were treated with control DMSO, or anti- α10β1 peptide (PGF) alone, Cisplatin alone or a combination of both. Tumor size was monitored by caliper measurements for 21 days. As shown in figure 4, Cisplatin (10.0mg/Kg), which was given twice per-week, inhibited SKOV-3 tumor growth. Interestingly, similar inhibition of tumor growth was initially observed with anti- α10β1 peptide PGF (10.0mg/Kg) given three times per week within the first 2 weeks, however, by 21 days the relative inhibition of tumor growth was less. Surprisingly, while no additive or synergistic effects were observed following combining Cisplatin and the PGF peptide (10.0mg/Kg), these preliminary studies suggest that targeting the α10β1 in SKOV-3 tumors may represent a novel strategy to regulate the growth of ovarian tumors in vivo. Additional experiments using a range of concentrations will be required to determine whether combining PGF-peptide may enhance the anti-tumor activity of Cisplatin. Given the limited anti-tumor activity observed at later time points, additional studies are underway to examine whether alterations in concentrations over time may result in the PGF-peptide acting as an agonists instead of an antagonist.

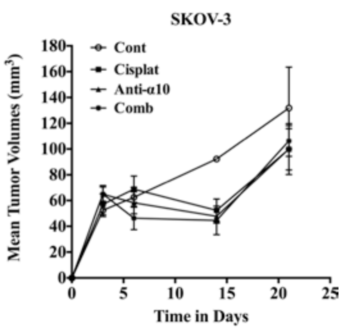

Figure 4. Effects of antagonists of α10β1 alone and in combination with Cisplatin on Ovarian tumor growth in vivo. Human SKOV-3 ovarian carcinoma cells ($3x10^6$/mouse) were injected in nude mice. Three days later mice were treated i.p with vehicle control (DMSO), Cisplatin (10mg/kg) alone, anti-α10β1 peptide PGF (10.0mg/kg) alone or a combination of both. Data bars represent mean tumor volumes ± standard errors from 6 mice per condition.

Histopathological analysis of tumors treated with antagonists of α10β1 alone and in combination with Cisplatin. As outlined in specific aim 1, we began to establish the working conditions for immunohistological quantification of cancer associated stromal cells including αSMA expressing fibroblasts infiltrates. As shown in figure 5 αSMA expressing stromal cells (red) were readily detected in control treated SKOV-3 tumors at the 21-day time point. Interestingly, a reduction in the relative levels of αSMA expressing stromal cells was observed in tumors in what appeared to be a distinct subset of cells as some isolated αSMA expressing cells still remained as small isolated groups scattered throughout the tumor. While quantification is clearly required, initial observations also suggest that Cisplatin had little effect on the infiltration of αSMA expressing cells. In fact, slightly enhanced levels were observed in these tumors as compared to controls, while tumors from the combination treated mice had a similar distribution of αSMA as was observed with tumors treated with PGF peptide alone.

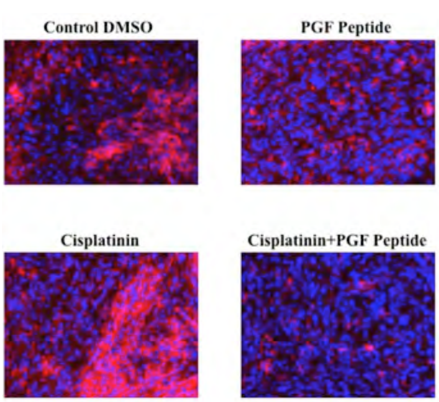

SKOV-3 ovarian carcinoma cells ($3x10^6$/mouse) were injected in nude mice. Three days later mice were treated i.p with vehicle control (DMSO), Cisplatin (10mg/kg) alone, anti-α10β1 peptide PGF (10.0mg/kg) alone or a combination of both. Frozen sections from each tumor were stained for expression of αSMA (Red). Photos (200x) represent examples from each experimental condition.

Effects of α10β1 in αSMA expressing fibroblasts on collagen adhesion. As outlined in aim 2, we sought to examine the effects of α10β1 expression in fibroblast may have on cell adhesion. To examine the functional significance of α10β1 on fibroblasts adhesion, we first knocked down expression of α10 integrin by shRNA. To confirm efficient knock down of α10 integrin whole cell lysates were prepared from fibroblasts transfected with shRNA directed to α10 integrin (α10-KD-HF) or a non-specific control (Con-KD-HF). As shown in figure 6A, little if any α10 integrin was detected in α10-KD-HF fibroblasts following western blot analysis. In contrast α10 integrin was readily detected in wild type and control transfected fibroblasts. Next we examined the fibroblast cell variants for their ability to attach to defined ECM substrates. Surprisingly, while the parental wild-type fibroblasts (WT) and control transfected cells (Con-K/D) readily attached to either intact native collagen (Figure 6B) or denatured collagen (Figure 6C), fibroblasts in which α10 integrin was knocked down exhibited enhanced adhesion. Addition experiments will be needed to confirm the significance of these surprising findings.

A. **B.** **C.**

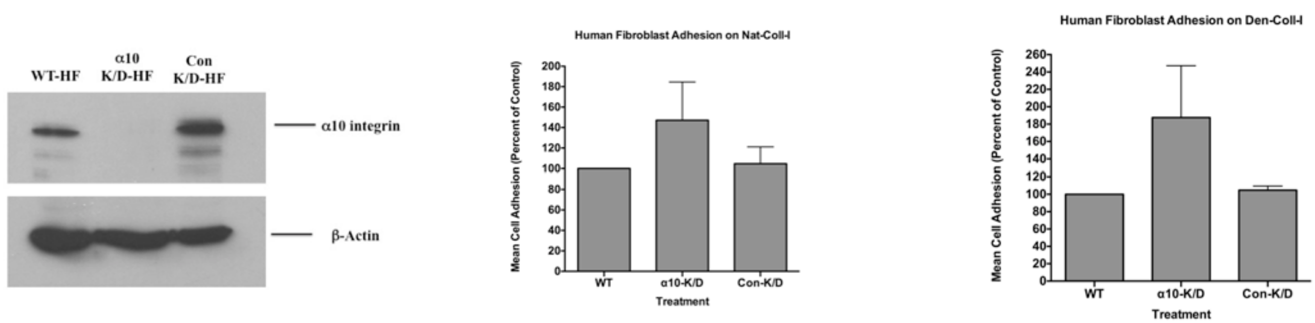

Figure 6. Effects of α10β1 in αSMA expressing fibroblasts on collagen adhesion. A). Wild type human fibroblasts (WT-HF) were transfected with shRNA specifically directed to α10 integrin (α10K/D-HF) or non-specific control (ConK/D-HF) and while cell lysates prepared. Western blot analysis indicates reduction of α10 integrin in α10 integrin (α10K/D-HF) cells. B). Quantification of fibroblasts variants attachment to native intact collagen. C). Quantification of fibroblasts variants attachment to denatured collagen. Data bars represent mean cell adhesion expressed as percent of control ± standard deviations from triplicate experiments.

Effects of α10β1 in αSMA expressing fibroblasts on collagen migration. As outlined in aim 2, we sought to examine the effects of α10β1 expression in fibroblast may have on cell migration. Fibroblast cell variants described above were allowed to migrate using transwell migration chambers coated with denatured collagen. As shown in figure 7, while the parental wild-type fibroblasts (WT) and control transfected cells (Con-K/D) readily migrated on denatured collagen, fibroblasts in which α10 integrin was knocked down exhibited significantly ($P<0.05$) reduced migration.

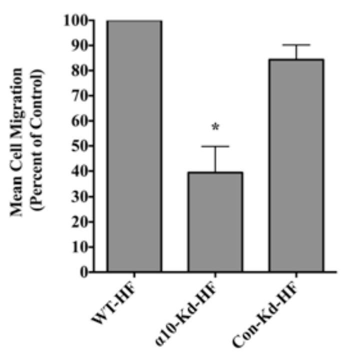

Figure 7. Effects of α10β1 in αSMA expressing fibroblasts on collagen migration. Integrin α10β1 expressing variants of human fibroblasts were seeded transwell membranes coated with denatured collagen and allowed to migrate for 2 hrs. Data bars represent mean cell migration indicated as percent of control from triplicate experiments. * $P<0.05$ as compared to controls.

Effects of α10β1 in αSMA expressing fibroblasts on proliferation. As outlined in aim 2, we sought to examine the effects of α10β1 expression in fibroblast may have on cell proliferation. To examine the functional significance of α10β1 on fibroblasts proliferation, fibroblast cell variants described above were allowed to proliferate for 24hrs on non-coated (Figure 8A), native collagen coated (Figure 8B), or denatured collagen coated micro-titer wells (Figure 8C). As shown in figure 8A-C, little if any change was observed in proliferation between control and α10 knock down cells among the different ECM substrate conditions. These data are consistent with notion that integrin α10 may play little if any direct role in fibroblasts proliferation under these experimental conditions.

A. **B.** **C.**

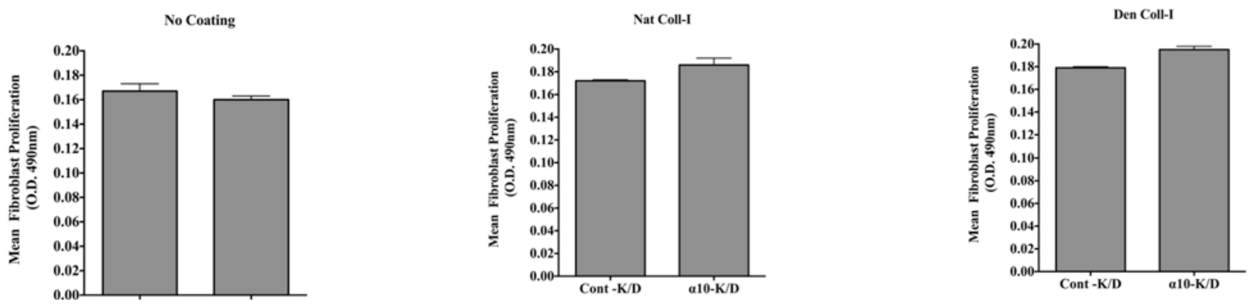

Figure 8. Effects of α10β1 in αSMA expressing fibroblasts on proliferation. Integrin α10β1 expressing fibroblasts variants were resuspended in proliferation buffer and seeded on microtiter wells that were either un-coated or coated with native collagen (Nat-Coll) or denatured collagen (Den-Coll). A). Quantification of cell proliferation on uncoated wells $\pm$ standard deviation from triplicate wells. B). Quantification of cell proliferation on native collagen coated wells $\pm$ standard deviation from triplicate wells. C). Quantification of cell proliferation on denatured collagen coated wells $\pm$ standard deviation from triplicate wells.

Effects of conditioned medium from αSMA positive α10β1 expressing fibroblasts on SKOV-3 tumor cell proliferation. As outlined in specific aim 2, we sought to examine the possible role of soluble growth factors and cytokines present in conditioned medium of α10β1 expressing fibroblasts on ovarian tumor cell growth. To begin these studies, we first examined the ability of concentrated serum free conditioned medium (CM) from α10β1 expressing fibroblasts to impact SKOV-3 ovarian tumor cell growth in vitro. As shown in figure 9A, addition of CM from α10β1 expressing fibroblasts to SKOV-3 ovarian tumor cells significantly ($P<0.05$) enhanced proliferation as compared to control CM prepared in the absence of the fibroblasts. To confirm the ability of fibroblast CM to enhance SKOV-3 cell growth we examined the relative levels of KI67 antigen levels between un-stimulated and CM stimulated SKOV-3 cells by western blot. As shown in figure 9B, enhanced levels of KI67 were detected in lysate from fibroblast CM stimulated SKOV-3 cell as compared to control. Taken together these findings are consistent with the presence of soluble factors within the CM from these fibroblasts to promote SKOV-3 ovarian tumor cell growth.

A. B.

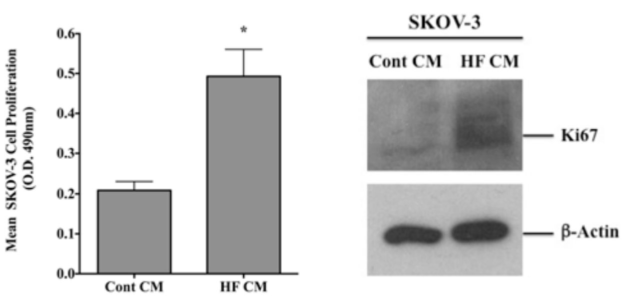

Figure 9. Effects of conditioned medium from αSMA positive α10β1 expressing fibroblasts on SKOV-3 tumor cell proliferation. A). SKOV-3 ovarian carcinoma cells were resuspended in the presence of serum free concentrated fibroblast conditioned medium (HF-CM) or concentrated medium prepared in the absence of fibroblasts (Cont-CM). SKOV-3 cells were allowed to proliferation for 24 hours. Data bars represent mean cell proliferation) $\pm$ standard deviations from triplicate wells. B). Western blot of whole cell lysates from SKOV-3 cells stimulated for 24 hours with Cont-CM or HF-CM and the levels of Ki67 antigen examined.

Cytokine profile of αSMA positive α10β1 expressing fibroblasts. As outlined in specific aim 2, we sought to examine the possible role of α10β1 integrin binding to the HU177 cryptic epitope in modulating the expression of cytokines that may regulate ovarian tumor growth. Given the effects concentrated serum free CM on SKOV-3 growth in vitro, we next sought to establish a basal cytokine expression profile in α10β1 expressing fibroblasts under basal culture conditions. To begin these studies, 24 hour concentrated serum free CM) was collected and analyzed for the expression of multiple cytokines using a Multi-Analyte ELISA assay kit. As shown in figure 10, an array of cytokines thought to modulate ovarian tumor cell growth and stromal cell infiltration were differentially expressed. These data are consistent with the ability of fibroblasts conditioned medium to alter the growth properties of the SKOV-3 ovarian carcinoma cells described above.

Cytokine	Positive Control	FB CM	Negative Control
IL-1α	1.857	0.471	0.058
IL-1β	2.607	0.491	0.068
IL-2	0.707	0.759	0.066
IL-4	1.448	0.692	0.062
IL-6	0.606	1.554	0.052
IL-8	3.292	3.785	0.043
IL-10	1.440	0.678	0.043
IL-12	1.780	0.877	0.053
IL-17A	1.670	2.747	0.053
TNF-α	0.564	0.435	0.040
INF-γ	1.089	1.490	0.045
GM-CSF	2.966	2.194	0.043

Figure 10. Cytokine profile of αSMA positive α10β1 expressing fibroblasts. Human fibroblasts (FB) were resuspended in serum free medium and allowed to incubate for 24 hours. Twenty-four hour serum free conditioned medium (CM) was collected and concentrated 10X. Concentrated fibroblast CM was analyzed for cytokine expression using a Multi-Analyte array ELISA.

Expression of Cytokines from α10β1 expressing fibroblasts attached to distinct ECM substrates. As outlined in specific aim 2, we sought to explore the possible role of α10β1 integrin-mediated binding to distinct forms of collagen might have on cytokine expression from fibroblasts. To this end, α10β1 expressing fibroblasts were seeded on either intact native collagen or denatured collagen under serum free conditions. Twenty-four hours later conditioned medium was collected and examined for differential expression of cytokines using a Multi-Analyte ELISA assay kit. As shown in figure 11, while the majority of cytokines examined showed little change between the distinct culturing conditions, a sharp reduction by nearly 2-fold in the levels of INFγ was observed in CM from fibroblasts cultured on denatured collagen as compared to intact native collagen.

Cytokine	Native Coll-1	Denatured Coll-I
IL-1α	0.398	0.385
IL-1β	0.436	0.436
IL-2	0.514	0.490
IL-4	0.430	0.468
IL-6	2.430	2.701
IL-8	3.621	3.606
IL-10	0.423	0.445
IL-12	0.544	0.436
IL-17A	1.729	1.862
INFγ	0.741	0.487
TNF-α	0.436	0.389
GM-CSF	0.991	0.719

Figure 11. Expression of Cytokines from α10β1 expressing fibroblasts attached to distinct ECM substrates. Human fibroblasts were resuspended in serum free medium and allowed to attach to either intact collagen coated wells or wells coated with denatured collagen for 24 hours. Twenty-four hour serum free conditioned medium (CM) was collected and concentrated 10X. Concentrated fibroblast CM was analyzed for cytokine expression using a Multi-Analyte array ELISA.

Characterization of α10 integrin expression in transgenic α10β1 knockout mouse model. As outlined in specific aim 1, we sought to examine the role of α10β1 integrin in regulating ovarian tumor growth in vivo. In this regard, we established a transgenic α10β1 integrin knockout mice in our laboratory. To confirm the status of the expression of α10 integrin in these mice genotyping was carried out on wild type, heterozygous and homozygous transgenic mice for α10 integrin (covering intron 6/7 and exon 8). As shown in figure 12A, while wild type and heterozygous mice expressed α10 integrin, we failed to detect $\alpha10\beta1$ in the homozygous mice. Moreover, the transgenic targeting construct, which included a LacZ gene and En2 cassette, which were readily detected in the homozygous mice. In addition, RT-PCR was carried out using isolated cartilage cells, a known source of α10 integrin. As shown in figure 12B, α10 integrin was readily detected in cells from wild type mice while we failed to detect α10 integrin in cartilage cells from homozygous knock out mice. These data confirm the utility of these transgenic mice as a $\alpha10\beta1$ integrin knockout model for our studies.

A. **B.**

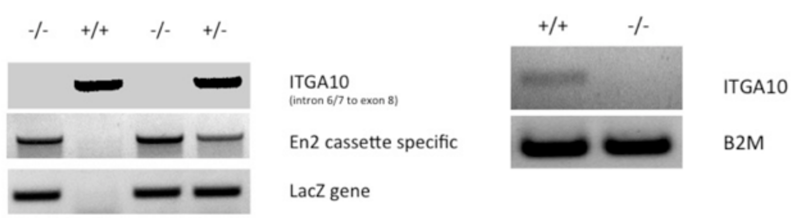

Figure 12. Characterization of α10 integrin expression in transgenic $\alpha10\beta1$ knockout mouse model. A). Genotyping analysis of wild type (+\+) heterozygous (+\-) and homozygous (-/-) transgenic α10 knock out mice for expression of α10 integrin, and the En2 cassette and Lac Z gene within the targeting construct. **B).** Expression (RT-PCR) of α10 integrin gene in cartilage cells isolated from wild type (+/+) and homozygous α10 knock out mice (-/-).

Characterization of ID8 ovarian tumors growing in wild type and α10 integrin knockdown mice. As outlined in specific aim 1, we sought to examine the growth and characterize ID8 ovarian tumors in mice in which integrin $\alpha10\beta1$ knocked down. To begin these studies, we first injected ID8 cell i.p into either wild type or homozygous transgenic α10 knock down mice. As shown in figure 13, i.p injection of ID8 tumor cells in wild type mice resulted in scattered small i.p tumors throughout the peritoneal cavity of the mice. Giemsa stain of these tumors growing in wild type mice indicated extensive stromal cell infiltration with multiple blood vessels (arrows). Interestingly, fewer ID8 tumor lesions were detected in α10 integrin knock down mice and while specific quantification will be needed, our preliminary analysis suggested that these ID8 tumors tended to be smaller in size. Moreover, these ID8 tumors also tended to have less stromal cell infiltration and fewer blood vessels. Further analysis and quantification will be needed to confirm these important preliminary observations.

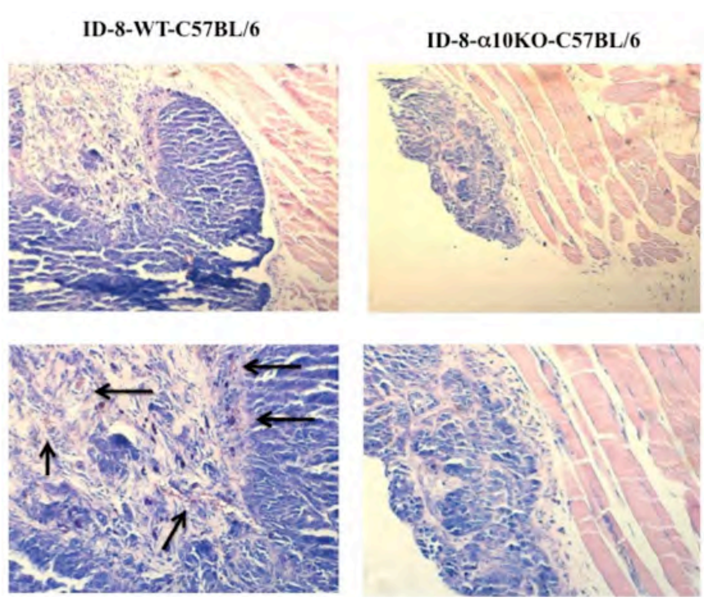

Figure 13. Characterization of ID8 ovarian tumors growing in wild type and α10 integrin knockdown mice. Wild type (+\+) left or homozygous (-/-) transgenic α10 knock out mice right were injected (i.p) with $5x10^6$ ID8 ovarian tumor cells. Tumors were allowed to grow for 6 weeks. Mice were sacrificed and i.p tumors were examined. Frozen sections of small i.p tumors (N=4) from each condition were stained by Giemsa for analysis. Top), representative examples of ID8 tumors (100x). Bottom), representative examples of ID8 tumors (200x). Arrows indicate tumor associated blood vessels.

What opportunities for training and professional development has the project provided? Nothing to report.

How were the results disseminated to communities of interest? Nothing to report.

What do you plan to do during the next reporting period to accomplish the goals?
We plan to complete the remaining studies proposed in our original pilot project. Briefly, we expect to complete our examination the effects of antagonists of α10β1 integrin alone and in combination with Cisplatin on murine ID8 tumors using the second C57BL/6 mouse model along with our novel transgenic α10 mouse model. In addition, we plan to complete our analysis of the effects of fibroblast mixing experiments on the growth of SKOV-3 and ID8 tumors in mice in vivo. Furthermore, we plan to complete our evaluation the effects of antagonists of α10β1 alone and in combination with Cisplatin on the relative levels of cytokines in the circulation in vivo. Finally, we plan to finish our evaluation of the effects of α10β1 has on stromal cell proliferation in vitro and its effects on cytokine expression in stromal cells in vitro. Collectively, these studies should complete the overall goal of our pilot project.

4). Impact
A). What was the impact on the development of the principal disciplines of the project? Our experimental results as detailed in this current report as well as our manuscript (see attached appendix), provides new insight into the role of a little understood integrin α10β1 on ovarian tumor growth. Specifically, our novel findings indicate that while α10β1 integrin is not highly expressed within the malignant ovarian tumor cells themselves, activated cancer associated fibroblasts that comprise a significant proportion of human malignant ovarian carcinomas express high levels of α10β1. Moreover, α10β1 expressed within these cancer associated stromal cells plays a functional role in their migration and accumulation within these ovarian tumors. Interestingly, conditioned medium from αSMA expressing fibroblasts enhanced the growth of SKOV-3 tumor cells consistent with the notion that this sub set of stromal cells may play an important role in ovarian tumor progression. Given the role of αSMA expressing stromal cells in regulating tumor growth, our novel findings are consistent with the possibility that blocking α10β1 integrin within the stromal compartment may have a therapeutic benefit for the treatment of ovarian cancer.

B). What was the impact on other disciplines? Given the high level of expression of integrin α10β1 expressed in αSMA positive tumor associated stromal cells and the role of αSMA expressing stromal cells in regulating many distinct tumor types, our novel findings are consistent with the possibility that blocking α10β1 integrin within the stromal compartment may have a therapeutic benefit for the treatment of a number of distinct cancers.

C). What was the impact on technology transfer? Nothing to report

D). What was the impact on society beyond science and technology? Nothing to report

5). Changes/Problems. Nothing to report.

6). Products:

A) A manuscript was prepared and was submitted for consideration for publication. (See attached in appendix).

Inhibition of ovarian tumor growth by targeting the HU177 cryptic collagen epitope.

Jennifer M. Caron, Jacquelyn, J. Ames, Liangru Contois, Leonard Liebes, Robert Friesel, Franco Muggia*, Calvin Vary, Leif Oxburgh, and +Peter C. Brooks. Maine Medical Center Research Institute, Center for Molecular Medicine, 81 Research Drive Scarborough Maine 04074. *NYU Langone Medical Center, Division of Hematology and Medical Oncology, 550 First Avenue, New York, NY 10016.

- **B)** Websites or Other Internet Sites: Nothing to Report
- **C)** Technologies or Techniques: Nothing to Report
- **D)** Inventions, patent applications, and/or licenses: Nothing to Report
- **E)** Other Products: Nothing to Report

7. Participants and Other Collaborating Organizations

Name	**Peter Brooks**
Project Role	**Principal Investigator**
Nearest Person Month Worked	**2.4 calendar months**
Contribution to Project	**Provides overall scientific direction, analysis, writes manuscripts, supervises lab technician**
Funding Support	

Name	**Jennifer Caron**
Project Role	**Laboratory Technician**
Nearest Person Month Worked	**4.8 calendar months**
Contribution to Project	**Conducted biochemical and animal experiments**
Funding Support	

Has there been a change in the active other support of the PD/PI or senior/key personnel since the last reporting period? Yes.
Maine Cancer Foundation grant received a no cost extension through 12/31/15.
DoD Grant CA093395 ended 8/31/14.

What other organizations were involved as partners? Nothing to report.

Special Reporting Requirements: n/a

APPENDIX: Submitted publication

Inhibition of ovarian tumor growth by targeting the HU177 cryptic collagen epitope.
Jennifer M. Caron, Jacquelyn, J. Ames, Liangru Contois, Leonard Liebes, Robert Friesel, Franco Muggia*, Calvin Vary, Leif Oxburgh, and +Peter C. Brooks. Maine Medical Center Research Institute, Center for Molecular Medicine, 81 Research Drive Scarborough Maine 04074. *NYU Langone Medical Center, Division of Hematology and Medical Oncology, 550 First Avenue, New York, NY 10016.

APPENDIX

Inhibition of ovarian tumor growth by targeting the HU177 cryptic collagen epitope.

Jennifer M. Caron, Jacquelyn, J. Ames, Liangru Contois, Leonard Liebes, Robert Friesel, Franco Muggia*, Calvin P. H. Vary, Leif Oxburgh, and +Peter C. Brooks. Maine Medical Center Research Institute, Center for Molecular Medicine, 81 Research Drive Scarborough Maine 04074. *NYU Langone Medical Center, Division of Hematology and Medical Oncology, 550 First Avenue, New York, NY 10016.

+To whom correspondence should be addressed: Peter C. Brooks, Ph.D., Maine Medical Center Research Institute, Center for Molecular Medicine, 81 Research Drive Scarborough, Maine 04074. Tel: (207) 396-8239; Fax: (207) 396-7669; Email: brookp1@mmc.org

Key Words: Extracellular matrix, Stroma, Collagen, Integrin $\alpha 10\beta 1$, P130Cas, Ovarian carcinoma, Cancer associated fibroblasts.

Running Title: HU177 epitope regulates ovarian tumor growth

Financial Support:

This work was supported by NIH grant CA91645 and an award from the Ovarian Cancer Research Program under award No. W81XWH-13-OCRP-PA to P.C.B. Additional support was from grants HL65301 (to R.F), HL083151 and AHA GRNT20460045 to (C.P.H.V.), a Chemotherapy Foundation grant to LL and grant P20 RR181789 (Bioinformatics Core) to D. M.Wojchowski. Additional support was from NIH 5P30GM103392 (PI: R. Friesel), ROIDK078161 to L.O and by institutional support from the MMC.

Financial Relationship: PCB, CPHV and LL hold an equity position in CryptoMedix, LLC.

Abstract.

Evidence suggests that stromal cells play critical roles in tumor growth. Uncovering new mechanisms that control stromal cell behavior and their accumulation within tumors may lead to development of more effective treatments for malignant cancers. Here we provide evidence that the HU177 cryptic collagen epitope is selectively generated within human ovarian carcinomas and this collagen epitope plays a functional role in SKOV-3 ovarian tumor growth in vivo. The ability of the HU177 epitope to regulate SKOV-3 tumor growth depends in part on its ability to modulate stromal cell behavior as targeting this epitope inhibited angiogenesis and surprisingly, the accumulation of αSMA expressing stromal cells. Integrin α10β1 can serve as a receptor for the HU177 epitope in αSMA expressing stromal cells and subsequently regulates p130Cas and Erk-dependent migration. These findings are consistent with a mechanism by which the generation of the HU177 collagen epitope provides a previously unrecognized α10β1-ligand that selectively governs angiogenesis and the accumulation of stromal cells, which in turn secrete pro-tumorigenic factors that contribute to ovarian tumor growth. Taken together, our findings provide new mechanistic understanding into the roles by which the HU177 epitope regulate ovarian tumor growth and provide new insight into the clinical results from a phase-I human clinical study of Mab D93/TRC093 in subjects with advanced malignant tumors.

Introduction

The importance of stromal cells such as endothelial cells, fibroblasts, pericytes and inflammatory infiltrates in tumor growth has been appreciated for years (1-4). This insight has led investigators to begin developing novel approaches to regulate stromal cell behavior (5-8). However, given the functions of stromal cells in normal physiological processes, it is important to create strategies that might restrict the impact on stromal cells to that within the tumor microenvironment. In this regard, the structures of extracellular matrix (ECM) proteins that compose the architectural framework of most normal tissues are largely intact. In contrast, tumors often exhibit an altered ECM structure with proteolytically degraded matrix proteins (9,10). This differential ECM configuration might provide a unique means for selectively regulating stromal cell behavior within tumors since cellular interactions with remodeled or denatured matrix proteins such as collagen alters adhesion, migration, proliferation and survival (11-14).

Our previous studies uncovered functional cryptic sites within ECM molecules (14-16). We have likened the process of generating cryptic elements to that of a biomechanical ECM switch, in which structural alterations in these molecules initiated by either proteolytic cleavage or other physical mechanisms leads to the generation of cryptic regulatory epitopes which contribute to the initiation of unique signaling cascades that facilitate angiogenesis, tumor growth and metastasis (11-17). Recently, we identified a new cryptic ECM epitope present within multiple forms of collagen (15). The HU177 epitope was generated within the ECM of angiogenic vessels and regulates endothelial cell behavior as a monoclonal antibody directed to this epitope inhibited endothelial cell adhesion and migration on denatured collagen and blocked angiogenesis in vivo (15). This antibody was humanized (Mab D93/TRC093) and a phase-I human clinical trial was completed (18-20). Clinical findings suggested that the HU177 epitope plays a role in tumor growth as 26% of the treated subjects exhibited stable disease and a reduction in liver lesions was observed in a subject with ovarian cancer (20).

Ovarian cancer is a heterogeneous disease classified by distinct histological subtypes (21-25). The molecular complexity of these tumors is demonstrated by the fact that low-grade type-I tumors often exhibit alterations in KRAS, BRAF and PTEN, while high-grade type-II tumors often have alterations in TP53 and BRCA1/2 (21-25). Importantly, stromal cells such as endothelial cells and activated fibroblasts may contribute to the development of ovarian carcinoma (26-28). While collagen remodeling occurs during ovarian tumor growth, it is not known whether these changes are sufficient to generate the HU177 epitope or what role it plays in ovarian tumor growth.

Here we present evidence that the HU177 cryptic collagen epitope is abundantly generated within human ovarian tumors, while little is expressed in benign granulomas. Antibodies directed to this epitope inhibited SKOV-3 tumor growth in vivo, which was accompanied by reductions in proliferation, angiogenesis and the accumulation of αSMA expressing stromal cells. While our studies indicate that α2β1 integrin can bind the HU177 site, the little understood integrin α10β1 plays an important role as a functional receptor in αSMA-expressing stromal cells. Inhibition of α10β1 or knock down of this integrin reduced phosphorylation of P130Cas and cellular migration in fibroblasts interacting with denatured collagen. Given the emerging roles of fibroblast-like cells in promoting tumor growth, these findings are consistent with a mechanism by which blocking the HU177 epitope reduces α10β1-dependent accumulation of αSMA expressing stromal cells, leading to the reduction of an important source of pro-tumorigenic cytokines that contribute to tumor progression.

Materials and Methods

Reagents, Chemicals and Antibodies. Collagen type-I was from Sigma (St Louis, MO). Fibroblast growth factor-2 (FGF-2), integrins $\alpha1\beta1$, $\alpha2\beta1$, $\alpha3\beta1$, $\alpha10\beta1$, $\alpha v\beta3$ and antibodies directed to $\alpha1$, $\alpha2$, αv integrins and IL-6 were from R&D Systems (Minneapolis, MN). Anti-CD-31 antibody was from BD Pharmingen (San Diego, CA). Anti-αSMA, anti-P130Cas and anti-Ki67 antibodies were from Abcam (Cambridge MA). Anti-Erk antibodies were from Cell Signaling Technology (Danvers, MA). Anti-collagen-I antibody was from Rockland (Gilbertsville, PA). Antibody to $\alpha10\beta1$ was from Novus Biologicals (Littleton CO). BrdU kit was from Millipore (Bedford, MA). Secondary antibodies were from Promega (Madison, WI). Mab HU177 was developed in our laboratory and shown to bind a PGxPG containing epitope exposed within denatured, but not intact collagen from multiple species (11-16). Mab D93/TRC093 is a humanized version of Mab HU177 that also binds the PGxPG containing epitope within denatured collagen from multiple species and was obtained from TRACON (San Diego, CA). The control antibody (Mab XL166) was generated in our laboratory and is directed to an RGD collagen epitope. Collagen PGF-peptide (CPGFPGFC) and Cont-peptides (CQGPSGAPGEC) and (CTWPRHHTTDALL) were from QED Biosciences (San Diego CA). MEK inhibitor (PD98059) was from CalBoichem (San Diego, CA).

*Analysis of tissue antigens***.** Human ovarian tissues were from MMC under IRB exempt protocol (No. 3175x). For quantification of the HU177 epitope, biopsies (N=9) from high-grade ovarian tumors (serous and endometrial) or benign ovarian granulomas (N=9) were stained with Mab HU177. For quantification, tissues were scanned using Kodak ID system and pixel density quantified from five 200x fields from each of 5 specimens from each condition using Molecular

Analyst Software ver 2.1 (29). Tumors were analyzed for apoptosis by TUNEL, proliferation using anti-Ki67 antibody (1:1000), angiogenesis using anti-CD31 antibody (1:300) and for CAF-like stromal cells using a combination of anti- αSMA (1:1000), anti-PDGF-Rα (1:500) and anti-FAP (1:300) antibodies. Quantification was performed within 5, 200X fields from each of 3 to 5 tumors.

Cells and Cell Culture. SKOV-3 cells, were from ATCC (Manassas, VA) and cultured in RPMI in the presence of 5% FBS. Human umbilical vein endothelial cells (HUVECs) were obtained from Lonza (Walkersville, MD) and cultured in EBM-2 medium in 2% FBS and supplements (Lonza). Human dermal fibroblasts were obtained from Science Cell (Carlsbad, CA) and cultured in medium with 2.0% FBS.

Solid-Phase Binding Assays. Plates were coated with 25µg/ml of native or denatured collagen. Collagen epitope peptide PGF and Cont-peptides were immobilized at 100ug/ml. Integrins (0-2.0µg/ml) were diluted in binding buffer as described (13). Integrins were allowed to bind for 1hr and plates washed and incubated with anti-integrin antibodies (1:100 dilution) for 1hr. Plates were washed and incubated with secondary antibodies (1:5000 dilution). In a second assay, integrins (0.5µg/ml) were coated and plates were washed, blocked as before and denatured collagen was added (0-10.0µg/ml). Denatured collagen was detected with anti-collagen antibody (1:1000). For integrin blocking ELISAs, wells were coated with denatured collagen and pre-treated (0.1µg/ml) with anti-HU177 or control antibody. Following washing, wells were incubated with integrins (2.0µg/ml) and binding was detected as described. Assays were carried out at least 3 times. For ELISA detection of HU177 epitope, conditioned medium (CM) from

Fibroblast, SKOV-3, and HUVEC was coated. The HU177 epitope was detected by ELISA using anti-HU177 antibody as described (15).

Cell Adhesion Assays. Wells were coated with 5μg/ml of native or denatured collagen. SKOV-3 and fibroblasts were suspended in adhesion buffer (13) and $1x10^5$ cells were added in the presence or absence of anti-HU177 or control antibodies (100μg/ml). Cells were allowed to attach for 25 minutes. Adhesion was quantified as described (15). Assays were completed at least 3x.

Cell Migration Assays. Membranes were coated with 5μg/ml of native or denatured collagen (15). Migration buffer in the presence or absence of 5X concentrated serum free SKOV-3 CM or 20ng/ml FGF-2 was placed in the lower chambers. SKOV-3 or fibroblasts (1×10^5) were resuspended in the presence or absence of antibodies directed to the HU177 epitope, or $\alpha 10\beta 1$, integrin (10μg/ml) or the MEK inhibitor (PD98054). Migration was quantified at 2 to 4 hrs by direct cell counts or by eluted dye (15). Assays were completed at least 3x.

Cell Proliferation Assays. To prepare serum free fibroblast CM, 2.0×10^6 cells were seeded in the presence of serum for 2hrs. Medium was removed and cells were washed and serum free RPMI was added. Serum free medium was collected at 24hrs and concentrated 10-fold. SKOV-3 cells were resuspended in the presence (150μl) of control (10X) RPMI or (10X) fibroblast CM. Cell proliferation was quantified at 24 or 72hrs using Brdu kit according to manufactures instructions. Assays were completed 3 times.

Tumor Growth Assays. Briefly, CAMs of 10-day chicks (N=6-8) were prepared as described (13) and SKOV-3 cells ($3x10^6$) were added (30) in the presence or absence of anti-HU177 antibody (100μg/embryo). Tumors were allowed to grow for 7 days and wet weights determined. For murine experiments, nude (NCRNU-F) mice (N=6-8) were injected with SKOV-3 cells ($3.0x10^6$/mouse). Mice were allowed to form tumors for 5 days then untreated or injected (i.p) with Mab D93 or control antibody (0-100μg/ml) 3x per week for 28 days. Tumors were measured with calipers and volumes calculated using the formula $V= L^2 x W/2$ were V= volume, L= length, W=width. Experiments were completed 3x.

Western Blot Analysis. Cells from culture or cells seeded on native or denatured collagen type-I were allowed to attach for 15 minutes then were lysed in RIPA buffer (Santa Cruz, CA) with 1X protease inhibitor cocktail. Lysates were separated by SDS PAGE and probed with antibodies directed to $\alpha10\beta1$, total and phosphorylated Erk, total and phosphorylated P130Cas, KI67 and β-tubulin or actin. Assays were performed at least 3 times.

Cytokine Analysis of Fibroblast CM. Serum free CM (50μl) was screened for a panel of 12 cytokines (IL-1α, IL-1β, IL-2, IL-4, IL-6, IL-8, IL-10, IL-12, IL-17A, TNF-α, INF-γ, GM-CSF) using the Multi-analyte ELISArray™ kit (Qiagen) according to manufactures instructions.

Statistical Analysis. Statistical analysis was performed using the InStat statistical program. Data analyzed for significance using Student T test. P values < 0.05 were considered significant.

RESULTS

Differential generation of the HU177 epitope in ovarian tumors. Studies have correlated enhanced collagen synthesis and ECM degradation with tumor progression (31,32). In this regard, we examined biopsies of human ovarian tumors and benign granulomas for expression of the HU177 cryptic collagen epitope. As shown in figure 1A, the HU177 epitope (green) could be detected in malignant ovarian tumors while minimal detection was observed in the benign ovarian lesions. Quantification of the relative levels of the HU177 epitope (Figure 1B) indicated a significant ($P<0.05$) increase in HU177 epitope in tumors as compared to the benign lesions. To confirm the generation of the HU177 epitope in an experimental mouse model, we examined its expression in SKOV-3 tumors growing in mice. As shown in figure 1C, while HU177 epitope was detected within SKOV-3 tumors little was observed in normal tissues including ovaries, liver and lungs. These findings are consistent with the restricted generation of the collagen epitope.

The HU177 epitope regulates ovarian tumor growth. Given the differential generation of the HU177 epitope observed in vivo, we sought to determine whether the HU177 epitope plays a functional role in ovarian tumor growth. To examine this possibility, SKOV-3 ovarian tumor cells were seeded on the chorioallantoic membrane (CAM) of chick embryos followed by treatment with anti-HU177 antibody or a non-specific control. As shown in figure 2A, SKOV-3 tumors dissected from chick embryos treated with anti-HU177 antibody were smaller than controls. Quantification indicated that targeting the HU177 epitope significantly ($P< 0.05$) inhibited SKOV-3 tumor growth by approximately 50% as compared to controls (Figure 2B). To confirm these findings in a murine model, SKOV-3 cells were injected into nude mice. Mice were either untreated or treated with anti-HU177 Mab or control antibody. As shown in figure 2C, treatment with anti-HU177 antibody significantly ($P<0.05$) reduced tumor size by approximately 70% by day 28. Dose dependent studies indicated inhibition of tumor growth at doses of anti-HU177 antibody as low as 10μg/mouse 3 times per week (data not shown).

The HU177 epitope regulates angiogenesis and stromal cell accumulation in ovarian tumors. The behavior of multiple cell types within the tumor microenvironment including stromal cells can be controlled by interactions with collagen (2,6,33-37). Therefore, we examined apoptosis within control and anti-HU177 treated SKOV-3 tumors using TUNEL staining. An approximately 1.8 fold increase in apoptosis was detected within anti-HU177 treated tumors as compared to control (data not shown), however, due to variation in staining, this increase did not meet statistical significance. Next we examined cellular proliferation by quantifying Ki67 antigen expression within these tumors. As shown in figure 3A, SKOV-3 tumors from anti-HU177 Mab treated mice exhibited significantly ($P<0.05$) reduced (25%-40%) Ki67 expression as compared to no treatment or control antibody respectively.

To examine the distribution of the HU177 epitope in ovarian tumors, SKOV-3 tumors were co-stained with antibodies directed to the HUI77 epitope and CD-31 a marker of blood vessels. While the HU177 epitope was detected in association with some CD-31 positive vessels (Figure 3B, top) it was more extensively associated with αSMA expressing fibroblast-like stromal cells (Figure 3B bottom). These observations prompted us to examine whether αSMA expressing fibroblasts, endothelial cells and/or SKOV-3 tumor cells might be associated with the generation of the HU177 epitope. To examine this possibility, ELISA assays were carried out to examine the relative levels of the HU177 epitope in serum free conditioned medium (CM) derived from

24 hour cultures of fibroblasts, HUVECs and SKOV-3 cells that were seeded on intact collagen. As shown in figure 3C, the HU177 epitope could be detected in CM from fibroblasts, HUVECs and SKOV-3 cells suggesting multiple cell types have the ability to generate the HU177 epitope. Given that activated fibroblasts express multiple enzymes capable of cleaving collagen, we assessed whether matrix metalloproteinase (MMPs) might play a role in its generation. As shown in figure 3D, incubation of fibroblasts with the MMP inhibitor GM6001 significantly ($P<0.05$) reduced the generation of the HU177 epitope by approximately 50% suggesting a role for MMPs in its generation. Confirming a role for MMPs in generating the HU177 epitope, incubation of purified collagen with either MMP-2 or MMP-9 also resulted in generation of the HU177 epitope (Data not shown). Collectively, these results are consistent with previous studies indicating a reduction in the generation of the HU177 epitope in MMP-9 null mice (16)

To further analyze the effects of anti-HU177 Mab treatment had on SKOV-3 tumors we next sought to quantify angiogenesis and the accumulation of αSMA expressing cells within SKOV-3 tumors. As shown in figure 3E, a significant ($P<0.05$) 35% inhibition of tumor angiogenesis was observed and remarkably, a 70% reduction in αSMA expressing stromal cells was also detected following treatment with anti-HU177 antibody (Figure 3F). These findings are consistent with the notion that reduced angiogenesis and αSMA expressing stromal cell accumulation may contribute to the anti-tumor activity observed following selective blockade of the HU177 collagen epitope.

The HU177 epitope regulates SKOV-3 and fibroblast adhesion and migration on denatured collagen. Tumor and fibroblast adhesive interactions with denatured collagen, which has been shown to be present within the microenvironment of malignant cancers, may regulate tumor progression. Therefore, we examined the impact of the HU177 epitope on SKOV-3 tumor cells and fibroblast adhesion. As shown in figure 4A and B, selectively blocking the HU177 epitope exposed within denatured collagen, significantly ($P<0.05$) inhibited adhesion of SKOV-3 and fibroblasts by 40% to 50% respectively. In contrast, targeting the HU177 epitope failed to inhibit adhesion to intact collagen (data not shown). These data indicate the ability of the anti-HU177 antibody to inhibit adhesion is restricted to those circumstances in which the HU177 epitope is generated and thus the anti-HU177 antibody does not alter adhesion to intact collagen thereby allowing a highly selective strategy to inhibit adhesive cellular interactions with collagen.

Next, we examined the migratory capacity of these cells. As shown in figure 4C and D, blocking the HU177 epitope exposed within denatured collagen also significantly ($P<0.05$) inhibited basal migration of SKOV-3 and fibroblasts by 35% to 38%, while migration on intact collagen was not effected (data not shown). While blocking the HU177 epitope inhibited adhesion and migration, it exhibited little direct effects on proliferation of SKOV-3 cells or fibroblasts in vitro (data not shown).

Inhibition of growth factor-induced fibroblast migration by targeting the HU177 epitope. Accumulating evidenced indicates that recruitment of activated and/or cancer-associated fibroblasts may facilitate tumor growth and survival, in part by providing an important source of pro-tumorigenic factors including IL-6 (2,5,6,38). While it is clear that most dermal fibroblast do not represent a fully accurate model of cancer associated stromal cells found in vivo, following in vitro culture, our fibroblasts exhibited phosphorylated Erk and expressed αSMA and PDGF-Rα (data not shown), important markers of CAF-like stromal cells. Therefore, we used these fibroblasts as a model of αSMA expressing stromal cells and examined whether blocking the HU177 epitope could alter growth factor-induced migration. As shown in figure 5A and B, concentrated SKOV-3 CM as well as recombinant FGF-2 stimulation enhanced migration on denatured collagen. Importantly, addition of the anti-HU177 antibody to the migration wells significantly ($P<0.05$) inhibited this growth factor stimulated response suggesting that not only can the HU177 epitope play a role in the basal cell migration, but also help regulate growth factor mediated motility.

Previous studies have indicated that FGF-2 stimulation can initiate a complex signaling cascade leading to the phosphorylation of multiple adaptor proteins including P130Cas, and additional effector molecules and transcription factors such as Erk1/2, which collectively help coordinate the complex events required for cellular migration (39-45). Given the role of P130Cas in coordinating cell motility mediated by ECM and growth factor stimulation, we examined whether fibroblast interactions with denatured collagen might alter P130Cas phosphorylation. As shown in figure 5C, the basal levels of phosphorylated P130Cas in the absence of any growth factor stimulation were enhanced by approximately 2-fold in cells attached to denatured collagen as compared to intact native collagen. These finding suggest that cellular interaction with a cryptic collagen epitope may enhance P130cas phosphorylation. To examine whether cellular interactions specifically with the HU177 epitope during growth factor stimulation alters P130Cas, fibroblasts were incubated with FGF-2 then plated on wells coated with denatured collagen or on wells in which the HU177 epitope was blocked by incubation with anti-HU177 antibody. As shown in figure 5D, while a small increase was observed in in P130Cas phosphorylation following FGF2 stimulation in cells attached to denatured collagen, blocking cellular interactions with the HU177 epitope inhibited P130cas phosphorylation below basal levels, suggesting the ability of the HU177 epitope to regulate P130Cas phosphorylation during FGF-2 stimulation.

Given the known role of FGF-2 and P130Cas in regulating Erk activation, we examined the effects of blocking fibroblast interactions with the HU177 epitope had on FGF-2 stimulated Erk phosphorylation. As shown in figure 5E, FGF-2 stimulated a small increase in Erk phosphorylation in cells attached to denatured collagen, while blocking the HU177 epitope reduced this phosphorylation. A mean reduction in Erk phosphorylation from 4 independent experiments of approximately 40% was observed (Figure 5F). To confirm a role for Mek/Erk signaling in FGF-2 stimulated fibroblast motility on denatured collagen, migration assays were carried out in the presence of a MEK inhibitor. As shown in figure 5G, addition of the MEK inhibitor (PD98059) significantly ($P<0.05$) blocked FGF-2 stimulated migration on denatured collagen suggesting a role for MAP/Erk signaling in regulating this migratory response.

Identification of β1-integrins as receptors for the HU177 epitope. We previously identified the repetitive PGxPG containing sequence as a critical component of the HU177 epitope (15). Given that variations of this motif are found throughout collagen, it is possible that a number of receptors bind to these cryptic sites. To this end, integrin receptors are an important class of molecules known to mediate cellular interactions with ECM components and coordinate signaling cascades that govern cell motility. To define potential cell surface receptors for HU177 collagen epitope, we examined the ability of various recombinant integrins to bind denatured collagen. Integrin α2β1 and αvβ3 dose dependently bound denatured collagen, while α1β1 showed minimal interactions (Figure 6A). Interestingly, integrin α10β1, a collagen binding receptor thought to have a limited tissue distribution outside of cartilage (46-49) also dose dependently bound denatured collagen. To confirm $\alpha10\beta1$ binding to denatured collagen we carried out a second binding assay by immobilizing $\alpha10\beta1$ on microtiter wells and examining soluble denatured collagen binding. Denatured collagen dose dependently bound $\alpha10\beta1$, but not $\alpha3\beta1$ (Figure 6B). To identify which integrins capable of binding denatured collagen have the ability to bind the HU177 epitope, we examined the effects of blocking the HU177 epitope on integrin binding. As shown in figure 6C, blocking the HU177 epitope inhibited $\alpha10\beta1$ binding by nearly 60%, while $\alpha2\beta1$ binding was reduced by approximately 30% (Figure 6D). Binding of $\alpha v\beta3$ to denatured collagen was unaffected (Figure 6E). To confirm the integrin binding specificity, direct binding to the synthetic PGxPG containing HU177 epitope (PGF peptide) was performed. As shown in figure 6F, while $\alpha2\beta1$ bound the HU177 epitope, $\alpha10\beta1$ exhibited 4-fold greater binding, while $\alpha v\beta3$ failed to bind. Moreover, the PGF-peptide also partially competed binding of $\alpha10\beta1$ to denatured collagen by approximately 60% (Figure 6G). Taken together, these findings suggest that the little understood integrin $\alpha10\beta1$ can bind the HU177 collagen epitope.

Integrin $\alpha10\beta1$ co-localizes with αSMA expressing cells in ovarian tumors. Given our studies indicating the ability of $\alpha10\beta1$ to bind the HU177 epitope, we examined the expression of $\alpha10\beta1$ within ovarian tumors. As shown in figure 7A, $\alpha10\beta1$ was detected within human ovarian tumors (left) and SKOV-3 tumors (right). Expression of $\alpha10\beta1$ was associated predominately with αSMA positive cells as suggested by extensive co-localization (Figure 7B). While minimal levels of $\alpha10$ protein (Figure 7C) and mRNA (data not shown) were detected in SKOV-3 cells, greater than 5 fold higher levels were detected in αSMA expressing fibroblasts.

We next examined the effects of blocking α10β1 on fibroblast migration. As shown in figure 7D, anti- α10 antibody inhibited FGF-2 stimulated migration on denatured collagen. To confirm a role for α10β1 integrin in fibroblast migration on denatured collagen, we knocked down expression α10β1 integrin in these fibroblasts using α10 specific shRNA and examined their ability to migrate on denatured collagen. As shown in figure 7E, while little if any change was observed in control transfected (Con-Kd-HF) fibroblasts as compared wild type parental cells (WT-HF), knocking down α10 integrin significantly ($P<0.05$) inhibited fibroblast migration on denatured collagen by approximately 60% as compared to controls.

Given these results, its possible that the reduction of αSMA positive stromal cells observed following anti-HU177 treatment leads to a reduction in an important source of pro-tumorigenic cytokines that facilitate tumor growth and angiogenesis. To this end, we examined whether CM from αSMA expressing fibroblasts might contain soluble factors that enhance SKOV-3 cell growth. As shown in figure 7E and F, fibroblast CM enhanced proliferation and Ki67 antigen expression in SKOV-3 cells. To characterize pro-tumorigenic factors expressed by these αSMA-positive fibroblasts, CM was screened using a multi-analyte cytokine array for expression of 12 different cytokines (data not shown). Among the cytokines that were expressed at the highest levels was IL-6. Interestingly, IL-6 has been shown to enhance growth of ovarian carcinoma cells (50,51), thus, we examined whether this pro-tumorigenic cytokine played a functional role in mediating the ability of αSMA expressing fibroblast CM to stimulate proliferation of SKOV-3 tumor cells. As shown in figure 7H, fibroblast CM significantly enhanced SKOV-3 tumor cell proliferation and a function-blocking antibody directed to IL-6 inhibited this response. These data are consistent with a role for IL-6 expression from fibroblasts in promoting SKOV-3 tumor cell growth. Taken together, these findings suggest the possibility that αSMA-expressing fibroblasts may serve as an important source of pro-tumorigenic factors that facilitate SKOV-3 tumor growth and that selectively reducing accumulation of αSMA expressing stromal cells by inhibiting the HU177 collagen epitope may contribute to the potent anti-tumor activity observed in vivo.

DISCUSSION

The array of mechanisms by which stromal cells such as endothelial cells and activated αSMA expressing fibroblasts govern the malignant phenotype are diverse and include providing proteolytic enzymes that alter the biomechanical properties of ECM, the release of pro-tumorigenic factors that act on both tumor and other cell types to alter their growth, survival and migratory behavior, and the release of molecules that influence the host immune response (1-6,52,53). Thus, selectively blocking the accumulation of pro-tumorigenic stromal cells in malignant lesions likely represents an important therapeutic strategy. While targeting stromal cells may provide a complementary strategy for tumor therapy, it remains challenging to selectively target them without disrupting their activity in normal tissues. The ECM represents an active control point for multiple mechanisms critical for regulating stromal cell behaviors ranging from migration and proliferation to gene expression (14). Therefore, inhibiting stromal cell-ECM interaction that selectively limit the accumulation of pro-tumorigenic stromal cells in malignant lesions might represent a useful strategy to control tumor progression.

Here we show that the HU177 collagen epitope is abundantly generated within ovarian carcinomas as compared to benign ovarian lesions. Interestingly, multiple cell types often found in tumors can generate the HU177 epitope. For example, αSMA-expressing fibroblast-like cells represent one important pro-tumorigenic cell type that generates the HU177 epitope in part by an

MMP-dependent mechanism. This cryptic collagen epitope played a role in SKOV-3 tumor growth and these findings are consistent with the recent clinical trial assessing tolerability and toxicity of Mab D93/TRC093 (20). Results from this study suggested no dose limiting toxicities and evidence of anti-tumor activity as a subject with an ovarian cancer showed a reduction in metastatic liver lesions (20). While all subjects eventually progressed, 26% exhibited disease stabilization and a subject with hemagiopericytoma, a tumor known to be highly infiltrated with stromal cells exhibited stable disease for nearly a year (20).

Consistent with previous findings (15,18) the anti-HU177 antibody inhibited tumor associated angiogenesis. These data are in agreement with previous studies indicating that targeting the HU177 epitope could selectively inhibit endothelial cell adhesion and migration on denatured collagen, inhibit proliferation, upregulates expression of P27KIP1 and inhibits angiogenesis (15). Surprisingly, our new studies now indicate that targeting the HU177 epitope can also reduce the accumulation of αSMA expressing stromal cells within SKOV-3 tumors. Targeting the HU177 epitope inhibited SKOV-3 and αSMA-expressing fibroblast adhesion and migration on denatured but not intact collagen, thereby specifically limiting the impact of this therapeutic agent to those tissues expressing the HU177 epitope. FGF-2 induced fibroblast migration on denatured collagen was shown to be dependent in part on MAP/Erk signaling as inhibition of MAP/Erk signaling blocked this migratory response.

Cell migration is governed by a complex and integrated set of signaling events that are coordinated in part by the unique composition and integrity of the local extracellular matrix. However, the mechanisms by which cells sense the structural changes in the integrity of a given ECM environment during tumor growth to facilitate cellular motility induced by growth factors are not completely understood. In fact, inappropriate and/or enhanced migration may contribute to tumor cell invasion and metastasis as well as the accumulation CAF-like stromal cells that contribute to tumor progression. In this regard, previous studies have suggested that the adaptor molecule P130Cas may function as a molecule switch to help coordinate the ability of cells to migrate following growth factor stimulation on defined ECM proteins including collagen (40-43). Integrin mediated interactions with ECM proteins are known to initiate assembly of a multiple-protein signaling complexes, which includes P130Cas. Phosphorylation of P130Cas within both its SH2 and SH3 domains facilitates protein-protein interactions that can coordinately regulate multiple down stream signaling cascades including Shc/Grab2/Ras and Fak/Src/Rap1 pathways that can activate MAPK/Erk signaling. (41). Our novel finding suggest that structural alterations in collagen which result in the generation of the HU177 epitope can enhance the phosphorylation of P130Cas and a function blocking antibody directed to this epitope inhibited P130Cas and Erk phosphorylation. It would be interesting to speculate that the selective generation of the HU177 epitope within the ovarian tumor microenvironment may help facilitate activation of the P130Cas molecular switch and Erk activation which may collectively promote stromal cell accumulation. While multiple protein kinases including members of the Src family kinases as well as Abl are thought to contribute to the phosphorylation of P130Cas, the precise molecular mechanism by which cellular interactions with the HU177 epitope regulates P130Cas phosphorylation is not known. Studies are currently underway to define which kinases and/or phosphatases might contribute to the enhance P130Cas phosphorylation following interactions with the HU177 collagen epitope.

Given the reduction in αSMA expressing cells in tumors treated with anti-HU177 antagonists, selectively inhibiting migration of this population of stromal cells may limit a major cellular source of pro-tumorigenic factors that play multiple roles in facilitate tumor cell survival and proliferation in vivo. In this regard, fibroblasts are known to express many pro-tumorigenic factors including IL-6, which has been previously shown to enhance proliferation of ovarian carcinoma cells (38,50,51). Consistent with these findings, our studies suggest that blocking IL-6 inhibited fibroblast CM-induced SKOV-3 cell growth. Given these findings and the high levels of IL-6 expressed by fibroblasts, our data is consistent with a mechanism by which targeting the HU177 epitope selectively limits accumulation of αSMA fibroblasts thereby reducing an important source of pro-tumorigenic factors that enhance angiogenesis and tumor growth.

Here we provide new evidence that the little understood integrin α10β1 functions as a receptor for the HU177 collagen epitope in fibroblasts. Given the variations within the HU177 PGxPG consensus site and the possibility of unique geometrical configurations displayed in vivo, it is possible that additional receptors may also recognize the HU177 epitope. Interestingly, little is known concerning the functions of α10β1 outside of chondrocytes and growth plate development (46-49). However, α10 mRNA has been detected in murine heart, muscle tissues and endothelial cells (46-49). Studies suggest that FGF-2 stimulation of mesenchymal stem cells (MSC) leads to upregulation of α10 integrin (54). Moreover, MSC have also been implicated as potential sources of αSMA expressing CAF-like cells in tumors (55). In addition, studies now suggest enhanced expression of α10β1 in melanoma cell lines as compared to primary melanocytes and inhibiting α10β1 in these cells resulted in a reduced migration (56).

Given the ability of α10β1 to bind the HU177 epitope, our data are in agreement with a novel mechanism by which generation of the HU177 epitope provides a previously unrecognized ligand for α10β1 expressing stromal cells that facilitates activation of P130Cas and Erk and subsequently the accumulation of αSMA positive stromal cells in ovarian tumors. In turn, the selective reduction in accumulation of this cell population by anti-HU177 antibody, in conjunction with its previously described anti-angiogenic effects likely contributes to its potent anti-tumor activity. Taken together our findings provide new cellular and molecular insight into the roles of the HU177 cryptic epitope in ovarian tumor growth and provide new mechanistic understanding of the therapeutic impact observed in human subjects treated with Mab D93 (20).

References:

1). Mursap, N, Diamandis, EP: Revisiting the complexity of the ovarian cancer microenvironment-clinical implications for treatment strategies. Mol Cancer Res 2012, 10: 1254-1264

2). Schauer, IG, Sood, AK, Mok, A, Liu, J: Cancer associated fibroblasts and their putative role in potentiating the initiation and development of epithelial ovarian cancer. Neoplasia 2011, 13: 393-405

3). Hanahan, D, Coussens, LM: Accessories to the crime: functions of cells recruited to the tumor microenvironment. Cancer Cell 2012, 21: 309-421

4). Qian, BZ, Pollard, JW: Macrophage diversity enhances tumor progression and metastasis. Cell 2010, 141: 39-51

5). Bansai, R, Tomar, T, Ostman, A, Poelstra, K, Prakash, J: Selective targeting of interferon γ to stromal fibroblasts and pericytes as a novel therapeutic approach to inhibit angiogenesis and tumor growth. Mol Cancer Ther 2012, 11: 2419-2428

6). Mitra, AK, Zillhardt, M, Hua, Y, Tiwari, P, Murmann, AE, Peter, ME, Lengyel, E: MicroRNAs reprogram normal fibroblasts into cancer-associated fibroblast in ovarian cancer. Cancer Discov 2012, 2: 1100-1108

7). Yao, Q, Qu, X, Yang, Q, Mingqian, W, Kong, B: CLIC4 mediates TGF-β1-induced fibroblast-to-myofibroblast trans differentiation in ovarian cancer. Oncol Reports 2019, 22: 541-548

8). Crawford, Y, Kasman, I, Yu, L, Zhong, C, Wu, X, Modrusan, Z, Kaminker J, Ferrara, N: PDGF-C mediates the angiogenic and tumorigenic properties of fibroblasts associated with tumors refractory to anti-VEGF treatment. Cancer Cell 2009, 15: 21-34

9). Ricciardelli, C, Rodgers, RJ: Extracellular matrix of ovarian tumors. Semin Reprod Med 2006, 24, 270-282

10). Capo-Chichi, CD, Smith, ER, Yang, DH, Roland, IH, Vanderveer, L, Hamiliton, TC, Godwin, AK, Xu, XX: Dynamic alterations of the extracellular matrix environment of ovarian surface epithelial cells in premalignant transformation, tumorigenicity, and metastasis. Cancer 2002 95, 1802-1815

11). Akalu, A, Roth, JM, Caunt, M, Policarpio, D, Liebes, L, Brooks, PC: Inhibition of angiogenesis and tumor metastasis by targeting a matrix immobilized cryptic extracellular matrix epitope in laminin. Cancer Res 2007, 67: 4353-4363

12). Hangai, M, Kitaya, N, Xu, J, Chan, CK, Kim, JJ, Werb, Z, Ryan, SJ, Brooks, PC: Matrix metalloproteinase-9-dependent exposure of a cryptic migratory control site in collagen is required before retinal angiogenesis. Am J Pathol 2002, 161: 1429-1437

13). Xu, J, Rodriguez, D, Petitclerc, E, Kim, JJ, Hangai, M, Yuen, SM, Davis, GE, Brooks, PC: Proteolytic exposure of a cryptic site within collagen type-IV is required for angiogenesis and tumor growth in vivo. J Cell Biol 2001, 154: 1069-1079

14). Cretu, A, Brooks, PC: Impact of the non-cellular microenvironment on metastasis: potential therapeutic and imaging opportunities. J Cell Physiol 2007, 213: 391-402

15). Cretu, A, Roth, JM, Caunt, M, Policarpio, D, Formenti, S, Gange, P, Liebes, L, Brooks, PC: Disruption of endothelial cell interactions with the novel HU177 cryptic collagen epitope inhibits angiogenesis. Clin Cancer Res 2007, 13: 3068-3078

16). Gagne, PJ, Tihonov, N, Li, X, Glaser, J, Qiao, J, Silberstein, M, Yee, H, Gagne, E, Brooks, PC: Temporal exposure of cryptic collagen epitopes within ischemic muscle during hindlimb reperfusion. Am J Pathol 2005, 167: 1349-1359

17). Ames, JJ, Vary, C PH, Brooks, PC**:** Signaling pathways and molecular mediators in metastasis. Biomechanical ECM Switches and Tumor Metastasis. Springer Press 2012, 3: 71-89

18). Pernasetti, F, Nickel, J, Clark, D, Baeurle, PA, Van Epps, D, Freimark, B: Novel anti-denatured collagen humanized antibody D93 inhibits angiogenesis and tumor growth: an extracellular matrix-based therapeutic approach. Int J Oncol 2006, 29: 1371-1379

19). Freimark, B, Clark, D, Pernasetti, F, Kickel, J, Myszka, D, Baeuerle, PA, van Epps, D: Targeting of humanized antibody D93 to sites of angiogenesis and tumor growth by binding to multiple epitopes on denatured collagens. Mol Immunol 2007, 44: 3741-3750

20). Robert, F, Gordon, MS, Rosen, LS, Mendelson, DS, Mulay, M, Adams, BJ, Alvare, D, Theuer, CP, Leigh, BR: Final results from a phase I study of TRC093 (humanized anti-cleaved collagen antibody) in patients with solid cancer. Annual meeting proceedings, 2010, *ASCO*. Abstract No 3038

21). Romero, I, Bast, RC: Minireview: human ovarian cancer: biology, current management, and paths to personalized therapy. Endocrinol 2012, 154: 1593-1602

22). Vaughan, S, Coward, JI, Bast, RC, Berchuck, A, Berek, JS, Brenton, JD, Coukos, G, Crum, CC, Drapkin, R, Etemadmoghadam, D, Friedlander, M, Gabra, H, Kaye, SB, Lord, CJ, Lengyel, E, Levine, DA, McNeish, IA, Menon, U, Mills, GB, Nephew, K, P, Oza, AM, Sood, AK, Stronach, EA, Walczak, H, Bowtell, DD, Balkwill, FR: Rethinking ovarian cancer: recommendations for improving outcomes. Nat Rev Cancer 2011, 11: 719-25

23). Kuman, RJ, Shih, M: The origin and pathogenesis of epithelial ovarian cancer: a proposed unifying theory. Am J Surg Pathol 2010, 34: 433-443

24). Kim, J, Coffey, DM, Creighton, CJ, Yu, Z, Hawkins, SM: High-grade serous ovarian cancer arises from fallopian tube in a mouse model. Proc Nat Acad Sci USA 2012, 109: 3921-3926

25). Ozols, RF, Bookman, MA, Connolly, DC, Daly, MB, Godwin, AK, Schilder, RJ, Xu, X, Hamilton, TC: Focus on epithelial ovarian cancer. Cancer Cell 2004 5: 19-24

26). Granot, D, Addadi, Y, Kalchenko, V, Harmelin, A, Kunz-Schugart, LA, Neeman, M: In vivo imaging of systemic recruitment of fibroblasts to the angiogenic rim of ovarian carcinoma tumors. Cancer Res 2007, 67: 9180-9190

27). Cai, J, Tang, H, Xu, L, Wang, X, Yang, C, Ruan, S, Guo, J, Hu, S, Wang, Z: Fibroblasts in omentum activated by tumor cells promote ovarian cancer growth, adhesion and invasiveness. Carcinogenesis 2013, 33: 20-29

28). Ko, SY, Barengo, N, Ladanyi, A, Lee, JS, Marini, F, Lengyel, E, Naora, H: HoxA9 promotes ovarian cancer growth by stimulating cancer-associated fibroblasts. J Clin Invest 2012, 122: 3603-3617

29). Roth, JM, Zelmanovich, A, Policarpio, D, Ng, B, MacDonald, S, Formenti, S, Liebes, L, Brooks, PC: Recombinant alpha 2(IV) NC1 domain inhibits tumor cell-extracellular matrix interactions, induces cellular senescence, and inhibits tumor growth in vivo. Am J Pathol 2005, 166: 901-911

30). Brooks, PC, Montgomery, AM, Rosenfeld, M, Reisfeld, RA, Hu, T, Klier, G, Cheresh, DA: Integrin αvβ3 antagonists promote tumor regression by inducing apoptosis of angiogenic blood vessels. Cell 1994, 79: 1157-1164

31). Zhu, GG, Melkko, J, Risteli, J, Kauppila, A, Risteli, L: Differential processing of collagen type-I and type III procollagens in the tumor cysts and peritoneal ascites fluid of patients with benign and malignant ovarian tumors. Clin Chim Acta 1994, 229: 87-97

32). Santala, M, Risteli, J, Risteli, L, Pulstola, U, Kacinski, BM, Stanley, ER, Kauppila, A: Synthesis and breakdown of fibrillar collagens: concomitant phenomena in ovarian cancer. Br J Cancer 1998, 77: 1825-1831

33). Kawamura, K, Komohara, Y, Takaishi, K, Katabuchi, H, Takeya, M: Detection of M2 macrophages and colony stimulating factor 1 expression in serous and mucinous ovarian epithelial tumors. Pathol International 59: 300-305

34). Cubillos-Ruiz, JR, Rutkowski, M, Conejo-Garcia, JR: Blocking ovarian cancer progression by targeting tumor microenvironmental leukocytes. Cell Cycle 2010, 9: 260-268

35). Petitclerc, E, Stromblad, S, von Schalscha, TL, Mitjans, F, Piulats, J, Montgomery, AM, Cheresh, DA, Brooks, PC: Integrin αvβ3 promotes M21 melanoma growth in human skin by regulating tumor cell survival. Cancer Res 1999, 59: 2724-2730

36). Anderberg, C, Pietras, K: On the origin of cancer-associated fibroblasts. Cell Cycle 2009, 8:1461-1465

37). Erez, N, Truitt, M, Olsen, P, Hanahan, D: Cancer-associated fibroblasts are activated in incipient neoplasia to orchestrate tumor-promoting inflammation in an NFκb-dependent manner. Cancer Cell 2010, 17: 135-147

38). Erez, N, Glanz, S, Raz, Y, Avivi, C, Barshack, I: Cancer associated fibroblasts express pro-inflammatory factors in human breast and ovarian tumors. Biochem Biophys Res Commun 2013, 437: 397-402

39). Cunningham, DL, Sweet, SMM, Cooper, HJ, Heath, JK: Differential phosphoproteomics of fibroblast growth factor signaling: identification of Src family kinase-mediated phosphorylation events. J Proteome Res 2010, 9: 2317-2328

40). Kanda, S, Miyata, Y, Kanetake, H, Smithgall, T, E: Fibroblast growth factor-2 induces the activation of Src through Fes, which regulates focal adhesion disassembly. Exp Cell Res 2006, 312: 3015-3022

41). Barberis, L, Wary, KK, Fiucci, G, Liu, F, Hirsch, E, Brancaccio, M, Altruda, F, Tarone, G, Giancotti, FG: Distinct roles of the adaptor protein Shc and focal adhesion kinase in integrin signaling to Erk. J Biol Chem 2000, 275: 36532-36540

42). Cho, AY, Klemke, RL: Extracellular-regulated kinase activation and CAS/Crk coupling regulate cell migration and suppress apoptosis during invasion of the extracellular matrix. J Cell Biol 2000, 149: 223-236

43). Sawada, Y, Tamada, M, Dubin-Thaler, BJ, Cherniavskaya, O, Sakai, R, Tanaka, S, Sheetz, M: Force sensing by mechanical extension of the Src family kinase substrate p130Cas. Cell 2006, 127: 1015-1026

44). Kottakis, F, Polytarchou, C, Foltopoulou, P, Sanidas, I, Kampranis, SC, Tsichlis, PN: FGF-2 regulates cell proliferation, migration and angiogenesis through an NDY1/KDM2B-miR-101-EZH2 pathway. Mol Cell 2011, 12: 285-298

45). Boilly, B, Vercoutter-Edouart, AS, Hondermarck, H, Nurcombe, V, Bourhis, XL: FGF signals for cell proliferation and migration through different pathways. Cytokine Growth Factor Rev 2000, 11: 295-302

46). Lehnert, K, Ni, J, Leung, E, Gough, S, Morris, CM, Liu, D, Wang, SX, Langley, R, Krissansen, GW: The integrin α10 subunit: expression pattern, partial gene structure, and chromosomal localization. Cytogent Cell Genet 1998, 87: 238-244

47). Bengtsson, T, Camper, L, Schneller, M, Lundgren-Akerlund, E: Characterization of the mouse integrin subunit α10 gene and comparison with its human homologue genomic structure, chromosomal localization and identification of splice variants. Matrix Biol. 2001, 20: 565-576

48). Bengtsson, T, Aszodi, A, Nicolae, C, Hunziker, EB, Lundgren-Akerlund, E, Fassler, R: Loss of α10β1 integrin expression leads to moderate dysfunction of growth plate chondrocytes. J. Cell Sci. 2004, 118: 929-936

49). Camper, L, Holmvall, K, Wangnerd, C, Asodi, A, Lundgren-Akerlund, E: Distribution of the collagen-binding integrin α10β1 during mouse development. Cell Tissue Res 2001, 306: 107-116

50). Wang, Y, Li, L, Jin, X, Sun, W, Zhang, X, Xu, RC: Interleukin-6 signaling regulates anchorage-independent growth, proliferation, adhesion and invasion in human ovarian cancer cells. Cytokine. 2012, 59: 228-236

51). Wang, Y, Xu, RC, Zhang, XL, Niu, XL, Qu, Y, Li, LZ, Meng, XY: Interleukine-8 secretion by ovarian cancer cells increases anchorage-independent growth, proliferation, angiogenic potential, adhesion and invasion. Cytokine. 2012, 59: 145-155

52). Santos, AM, Jung, J, Aziz, N, Kissil, JL, Pure, E: Targeting fibroblast activation protein inhibits tumor stromagenesis and growth in mice. J Clin Invest 2009, 119: 3613-3625

53). Kraman, M, Bambrough, PJ, Arnold, JN, Roberts, EW, Magiera, L, Jones, JO, Gopinathan, A, Tuveson, DA, Fearon, DT: Suppression of anti-tumor immunity by stromal cells expressing fibroblast activation protein-α. Science 2001, 250: 827-830

54). Varas, L, Ohlsson, LB, Honeth, G, Olsson, A, Bengtsson, T, Wiberg, C, Bockermann, R, Järnum, S, Richter, J, Pennington, D, Johnstone, B, Lundgren-Akerlund, E, Kjellman, C: α10 integrin expression is upregulated on fibroblast growth factor-2-treated mesenchymal stem cells with improved chondrogenic differential potential. Stem Cell Develop 2007, 16: 965-978

55). Mishra, PJ, Mishra PJ, Glod, JW, Banerijee, D: Mesenchymal stem cells: flip side of the coin. Cancer Res 2009, 69: 1255-1258.

56). Wenke, AK, Kjellman, C, Lundgren-Akerlund, E, Uhlmann, C, Haass, NK, Herlyn, M, Bosserhoff, AK: Expression of integrin α10 is induced in malignant melanoma. Cell Oncol 2007, 29: 373-386

Figure Legends.

Figure 1. Generation of the HU177 epitope in ovarian tumors. Biopsies from human ovarian tumors or benign granulomas were stained with anti-HU177 antibody. A). Examples of HU177 epitope (green) from each tissue. B). Data bars represent the mean relative levels of HU177 epitope $\pm$ S.E from five 200X fields. * $P<0.05$ as compared to controls. C). Examples of HU177 epitope (red) within SKOV-3 tumors, or normal ovaries, lungs and liver. Photos were at 200X. Scale bar 63 microns.

Figure 2. Inhibition of tumor growth by targeting the HU177 epitope. A and B). SKOV-3 cells were seeded on CAMs of chick embryos. Animals were untreated (NT) or treated (100ug) with anti-HU177 or control antibody. A). Examples of tumors from each condition. B). Data bars represent mean tumor weights $\pm$ S.E. C). Mice were injected with SKOV-3 cells and 5 days later were untreated or treated (100ug) with anti-HU177 antibody or control antibody. Data points represent mean tumor volume $\pm$ SE. * $P<0.05$ as compared to controls.

Figure 3. Analysis of SKOV-3 tumors. Mice were injected with SKOV-3 cells and untreated or treated with anti-HU177 or control antibodies. A). Analysis of the relative levels of Ki67 expression per 200X field $\pm$ SE in SKOV-3 tumors. B Top). Co-expression of CD-31 (green) and HU177 epitope (red) in SKOV-3 tumors. B Bottom). Co-expression of αSMA (red) and HU177 epitope (green) in SKOV-3 tumors. C). Quantification of the relative levels HU177 epitope in CM from distinct cell types $\pm$ SE. D). Quantification of HU177 epitope in CM from fibroblast in the presence of MMP inhibitor GM6001 $\pm$ SE. E and F). Mice were injected with SKOV-3 cells and untreated or treated (100ug) with anti-HU177 or control antibody. E). Top,

examples of tumors from each condition stained for CD-31 (red). Bottom, data bars represent mean vessels per 100X field $\pm$ SE. F). Top, examples of tumors from each condition stained for αSMA (red). Bottom). Data bars represent mean αSMA expression per 100X field $\pm$ SE. Scale bar 126 microns. * $P<0.05$ as compared to controls.

Figure 4. Blocking the HU177 epitope inhibits basal adhesion and migration on denatured collagen. SKOV-3 cells (A and C) and fibroblasts (B and D) were resuspended in the presence or absence anti-HU177 or control antibody. A and B). Data bars represent mean cell adhesion indicated as percent of control$\pm$ SE from 3 experiments. C and D). Data bars represent mean cell migration indicated as percent of control$\pm$ SE from 3 experiments. * $P<0.05$ as compared to controls.

Figure 5. Targeting the HU177 epitope inhibits growth factor induced migration, P130cas and Erk phosphorylation. Fibroblasts were resuspended in the presence or absence of SKOV-3 CM (A) or FGF-2 (B) in the presence or absence of anti-HU177 or control antibodies. A and B). Data bars represent mean migration indicated as percent of control$\pm$ SE from 3 experiments. C). Western blot analysis of total (t-P130Cas) or phosphorylated P130Cas (p-P130Cas) in lysates from fibroblasts seeded on native (Nat) or denatured (Den) collagen. D). Western blot analysis of total (t-P130Cas) or phosphorylated P130Cas (p-P130Cas) in lysates from non-stimulated or FGF-2 stimulated fibroblasts seeded on denatured collagen which was either not treated or pre-blocked with anti-HU177 antibody or non-specific control antibody. E). Western blot analysis of Erk in lysates from fibroblasts seeded on denatured collagen in the presence or absence of anti-HU177 or control antibody. F). Quantification of mean Erk phosphorylation from 4

independent experiments. G). Fibroblasts were resuspended in the presence or absence of FGF2 and in the presence or absence of Mek inhibitor. Data bars indicate mean cell migration indicated as percent of control$\pm$ SE from 3 experiments. * $P<0.05$ as compared to controls.

Figure 6. Integrin $\alpha 10\beta 1$ binds the HU177 collagen epitope. Wells were coated with denatured collagen (A, and C-E), integrins $\alpha 10\beta 1$ and $\alpha 3\beta 1$ (B) or the synthetic HU177 epitope peptide or control peptide (F) and integrins (A, C-E) or denatured collagen (B) and allowed to bind. A). Integrin binding to denatured collagen. B). Binding of denatured collagen to immobilized integrins. C). Binding of $\alpha 10\beta 1$ to denatured collagen in the presence or absence of anti-HU177 or control antibodies. D). Binding of $\alpha 2\beta 1$ to denatured collagen in the presence or absence of anti-HU177 or control antibodies. E). Binding of $\alpha V\beta 3$ to denatured collagen in the presence or absence of anti-HU177 or control antibodies. F). Integrin binding to synthetic HU177 epitope or control peptide. G). Integrin binding to denatured collagen in the presence of synthetic HU177 epitope or control peptide. Experiments were completed at least 3 times. * $P<0.05$ as compared to controls.

Figure 7. Expression and migratory function of $\alpha 10\beta 1$ in ovarian tumors. A). Expression of $\alpha 10\beta 1$ (green) in human ovarian tumor biopsy (left) and SKOV-3 tumors (right). B). Co-expression of $\alpha 10\beta 1$ (green) and αSMA (red) expressing stromal cells within SKOV-3 tumors. Photos were at 200X. C). Analysis of $\alpha 10\beta 1$ expression in SKOV-3 cells or fibroblasts (HF) by western blot. D). Quantification of FGF-2-induced fibroblasts migration in the presence or absence of anti- $\alpha 10\beta 1$ antibody or control. Data bars represent mean migration indicated as percent of control$\pm$ SE from 3 experiments. E). Quantification of FGF-2-induced migration of

wild type (WT-HF), α10 integrin knock down fibroblasts (α10-Kd-HF) or non-specific control transfected fibroblasts (Con-Kd-HF) on denatured collagen. Data bars represent mean migration indicated as percent of control$\pm$ SE from 3 experiments. F). SKOV-3 proliferation in the presence of control or fibroblast CM. Data bars represent mean O.D 490nm $\pm$ SE. G). Western analysis for Ki67 in lysates of SKOV-3 cells treated with fibroblast CM. H). SKOV-3 proliferation in the presence or absence of fibroblast CM and in the presence of anti-IL-6 or control antibodies. Data bars represent mean O.D 490nm $\pm$ SE. All experiments were completed at least 3 times with similar results. Scale bar 63 microns. * $P<0.05$ as compared to controls.

Figure 1.

A.

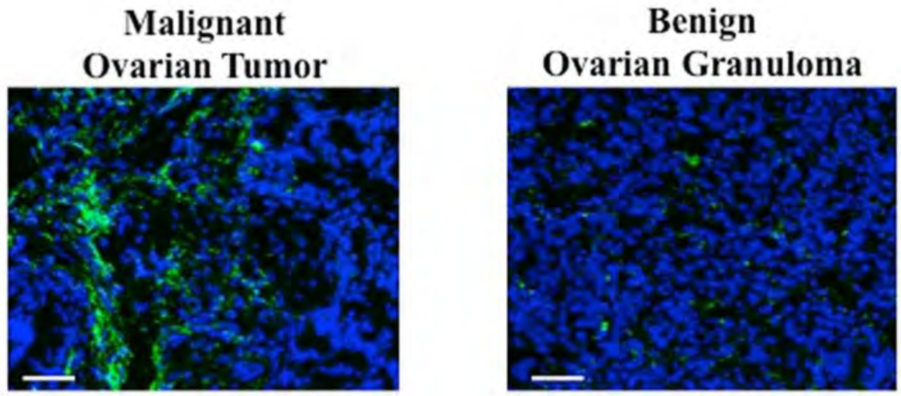
Malignant
Ovarian Tumor
Benign
Ovarian Granuloma

B.

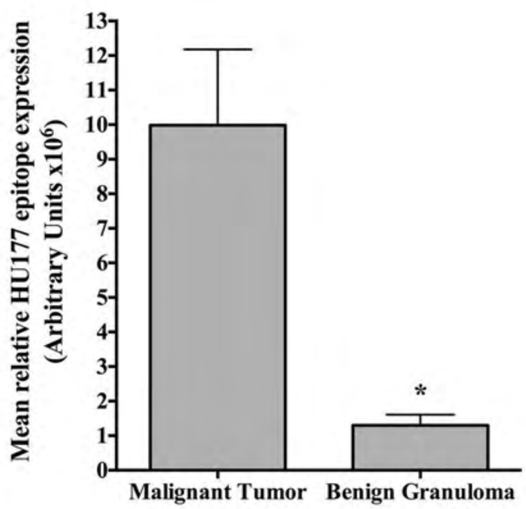
Mean relative HU177 epitope expression
(Arbitrary Units x10^6)
13
12
11
10
9
8
7
6
5
4
3
2
1
0
*
Malignant Tumor
Benign Granuloma

C.

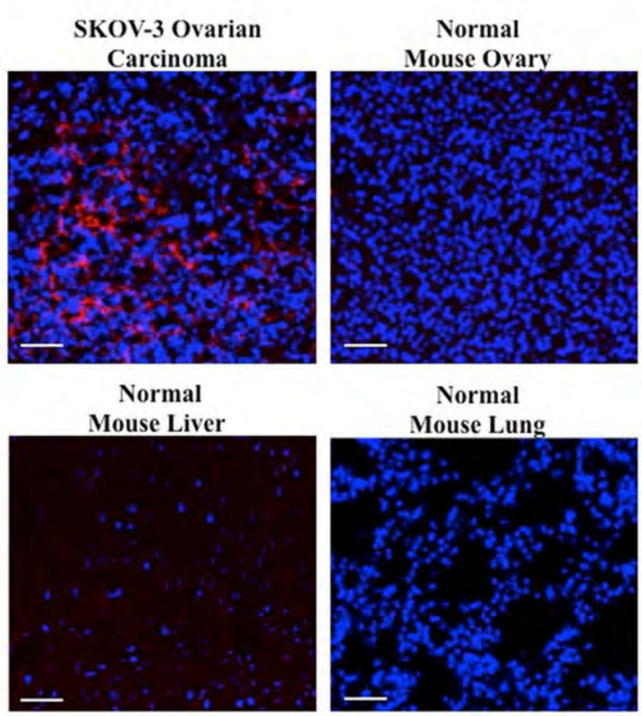
SKOV-3 Ovarian
Carcinoma
Normal
Mouse Ovary
Normal
Mouse Liver
Normal
Mouse Lung

Figure 2.

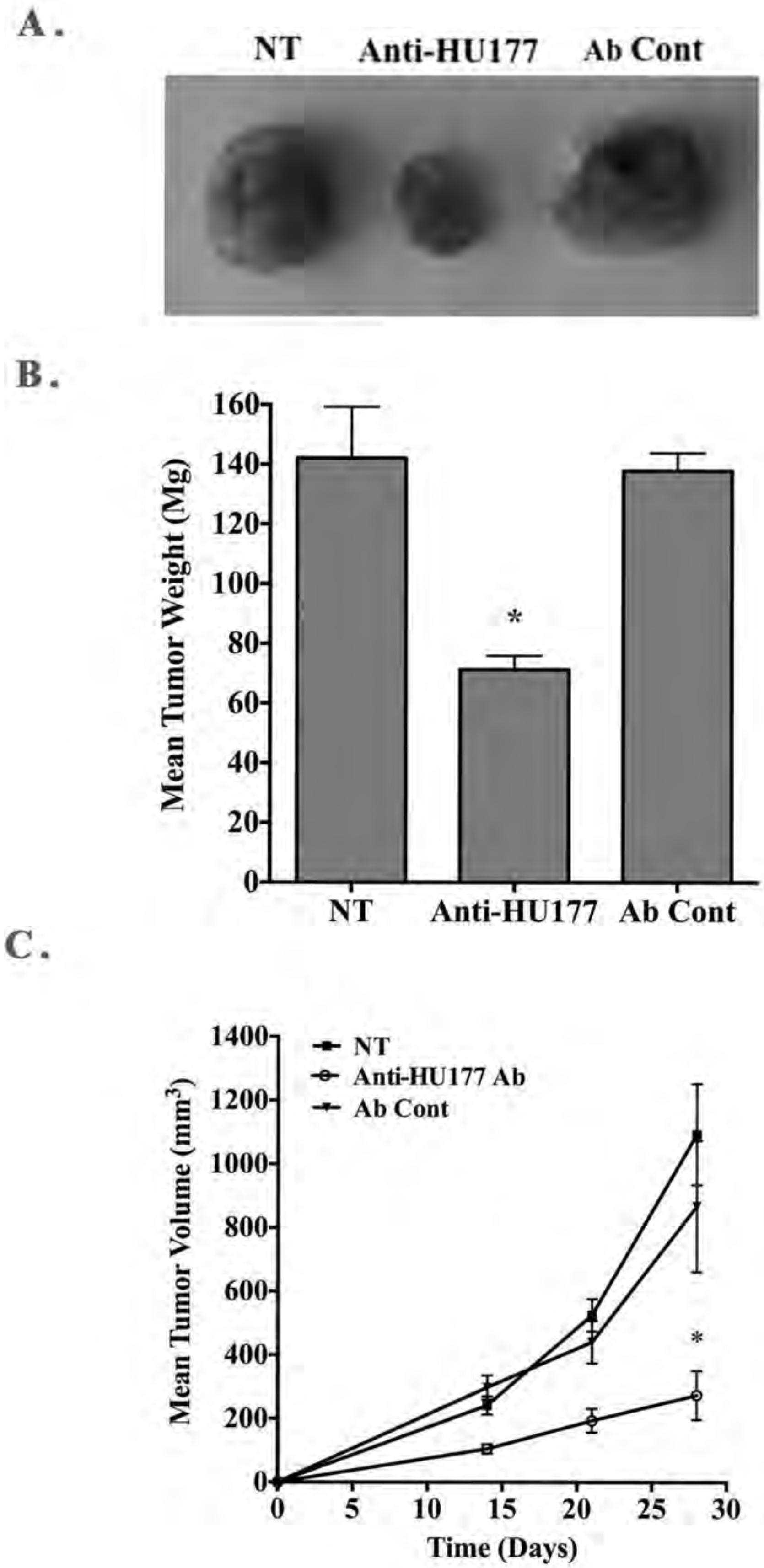
A.
NT
Anti-HU177
Ab Cont
B.
Mean Tumor Weight (Mg)
0
20
40
60
80
100
120
140
160
*
NT
Anti-HU177
Ab Cont
C.
Mean Tumor Volume (mm^3)
0
200
400
600
800
1000
1200
1400
NT
Anti-HU177 Ab
Ab Cont
*
0
5
10
15
20
25
30
Time (Days)

Figure 3.

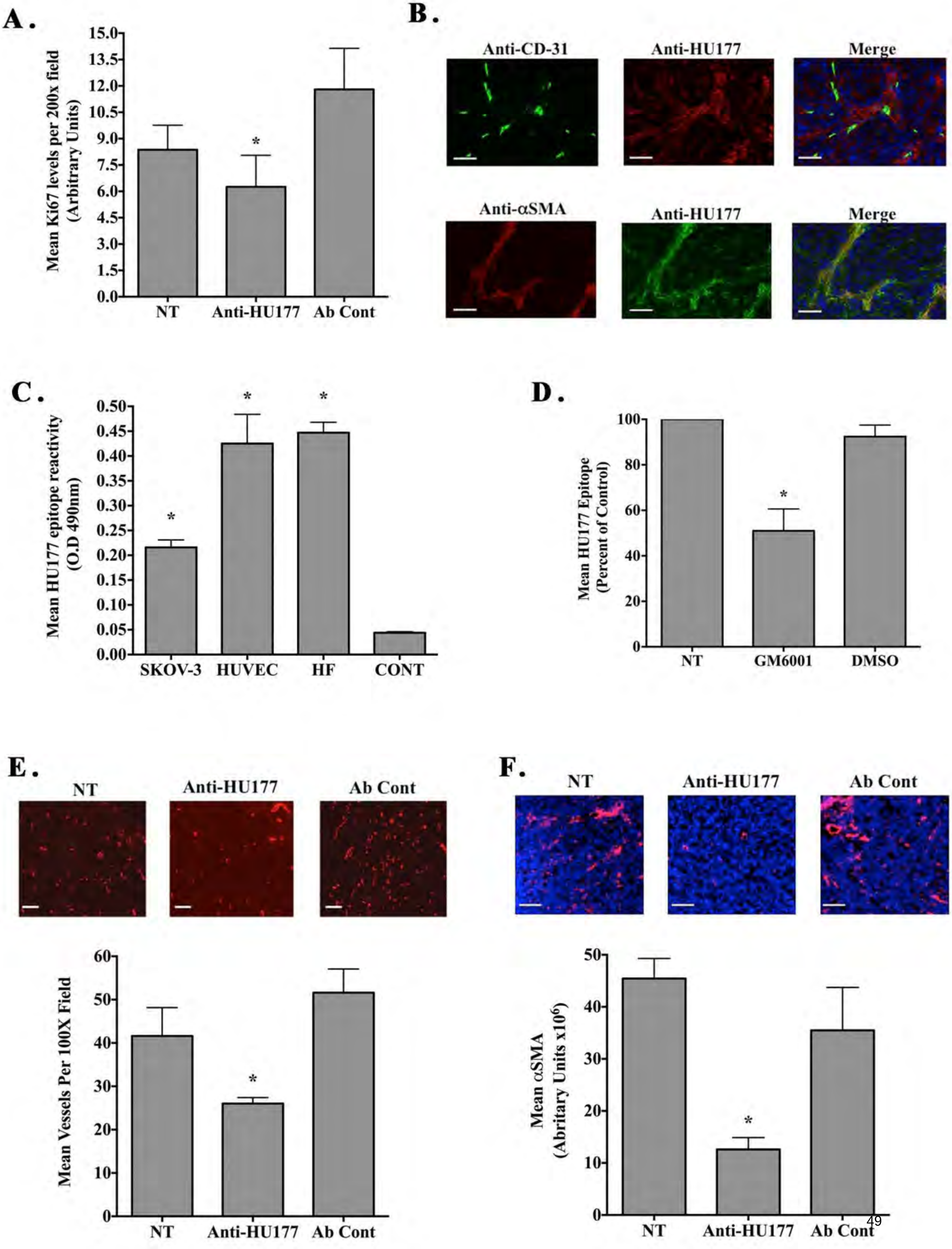
A.
Mean Ki67 levels per 200x field (Arbitrary Units)
15.0
13.5
12.0
10.5
9.0
7.5
6.0
4.5
3.0
1.5
0.0
*
NT
Anti-HU177
Ab Cont
B.
Anti-CD-31
Anti-HU177
Merge
Anti-αSMA
Anti-HU177
Merge
C.
Mean HU177 epitope reactivity (O.D 490nm)
0.50
0.45
0.40
0.35
0.30
0.25
0.20
0.15
0.10
0.05
0.00
*
*
*
SKOV-3
HUVEC
HF
CONT
D.
Mean HU177 Epitope (Percent of Control)
100
80
60
40
20
0
*
NT
GM6001
DMSO
E.
NT
Anti-HU177
Ab Cont
Mean Vessels Per 100X Field
60
50
40
30
20
10
0
*
NT
Anti-HU177
Ab Cont
F.
NT
Anti-HU177
Ab Cont
Mean αSMA (Abritary Units x10⁶)
50
40
30
20
10
0
*
NT
Anti-HU177
Ab Cont

Figure 4.

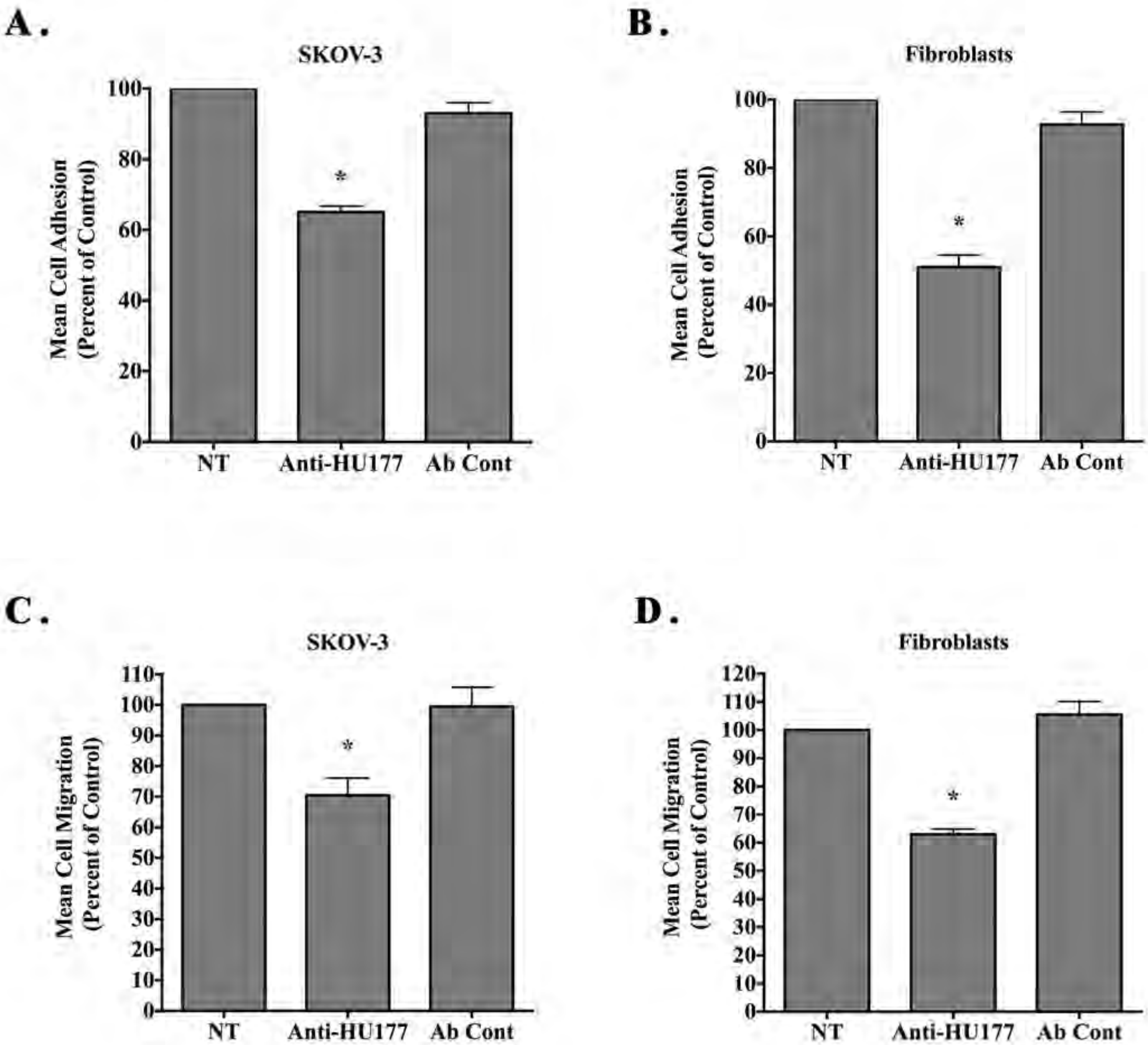
A.
SKOV-3
Mean Cell Adhesion (Percent of Control)
0
20
40
60
80
100
NT
Anti-HU177
Ab Cont
*
B.
Fibroblasts
Mean Cell Adhesion (Percent of Control)
0
20
40
60
80
100
NT
Anti-HU177
Ab Cont
*
C.
SKOV-3
Mean Cell Migration (Percent of Control)
0
10
20
30
40
50
60
70
80
90
100
110
NT
Anti-HU177
Ab Cont
*
D.
Fibroblasts
Mean Cell Migration (Percent of Control)
0
10
20
30
40
50
60
70
80
90
100
110
120
NT
Anti-HU177
Ab Cont
*

Figure 5.

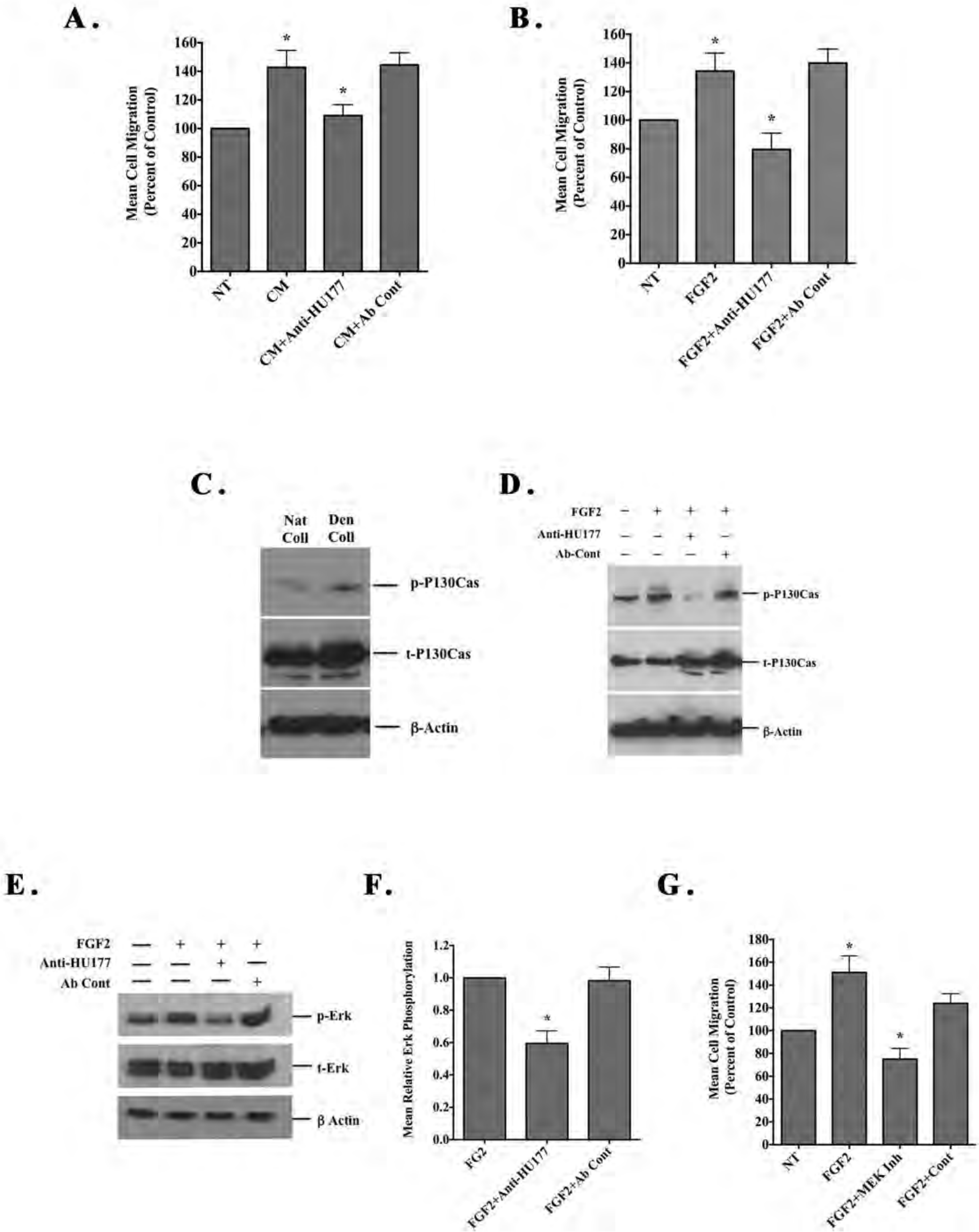

A.
Mean Cell Migration (Percent of Control)
NT
CM
CM+Anti-HU177
CM+Ab Cont
B.
Mean Cell Migration (Percent of Control)
NT
FGF2
FGF2+Anti-HU177
FGF2+Ab Cont
C.
Nat Coll
Den Coll
p-P130Cas
t-P130Cas
β-Actin
D.
FGF2
Anti-HU177
Ab-Cont
p-P130Cas
t-P130Cas
β-Actin
E.
FGF2
Anti-HU177
Ab Cont
p-Erk
t-Erk
β Actin
F.
Mean Relative Erk Phosphorylation
FG2
FGF2+Anti-HU177
FGF2+Ab Cont
G.
Mean Cell Migration (Percent of Control)
NT
FGF2
FGF2+MEK Inh
FGF2+Cont

Figure 6.

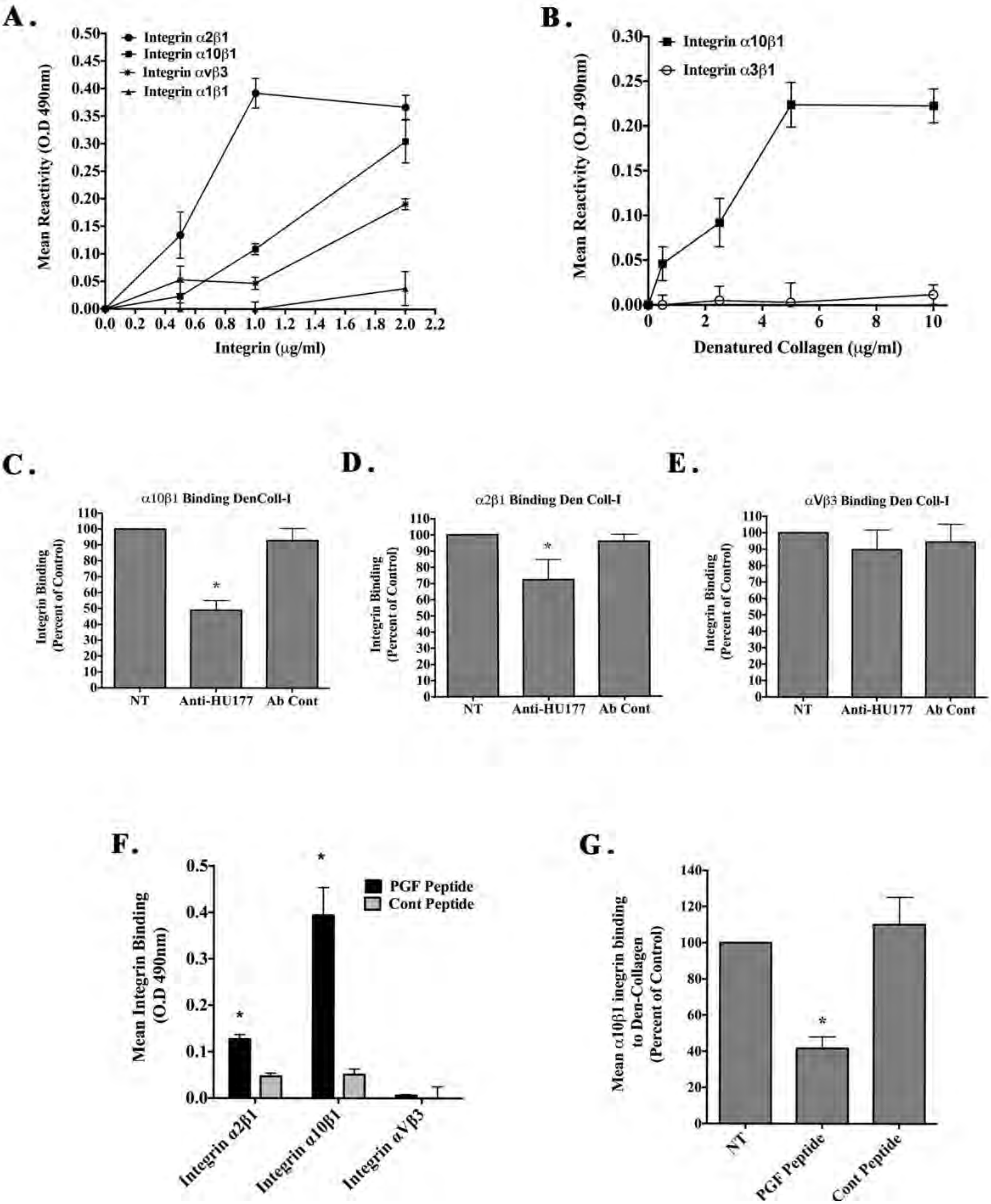

A.
Integrin α2β1
Integrin α10β1
Integrin αvβ3
Integrin α1β1
Mean Reactivity (O.D 490nm)
Integrin (μg/ml)
B.
Integrin α10β1
Integrin α3β1
Mean Reactivity (O.D 490nm)
Denatured Collagen (μg/ml)
C.
α10β1 Binding DenColl-I
Integrin Binding (Percent of Control)
NT
Anti-HU177
Ab Cont
D.
α2β1 Binding Den Coll-I
Integrin Binding (Percent of Control)
NT
Anti-HU177
Ab Cont
E.
αVβ3 Binding Den Coll-I
Integrin Binding (Percent of Control)
NT
Anti-HU177
Ab Cont
F.
PGF Peptide
Cont Peptide
Mean Integrin Binding (O.D 490nm)
Integrin α2β1
Integrin α10β1
Integrin αVβ3
G.
Mean α10β1 inegrin binding to Den-Collagen (Percent of Control)
NT
PGF Peptide
Cont Peptide

Figure 7.

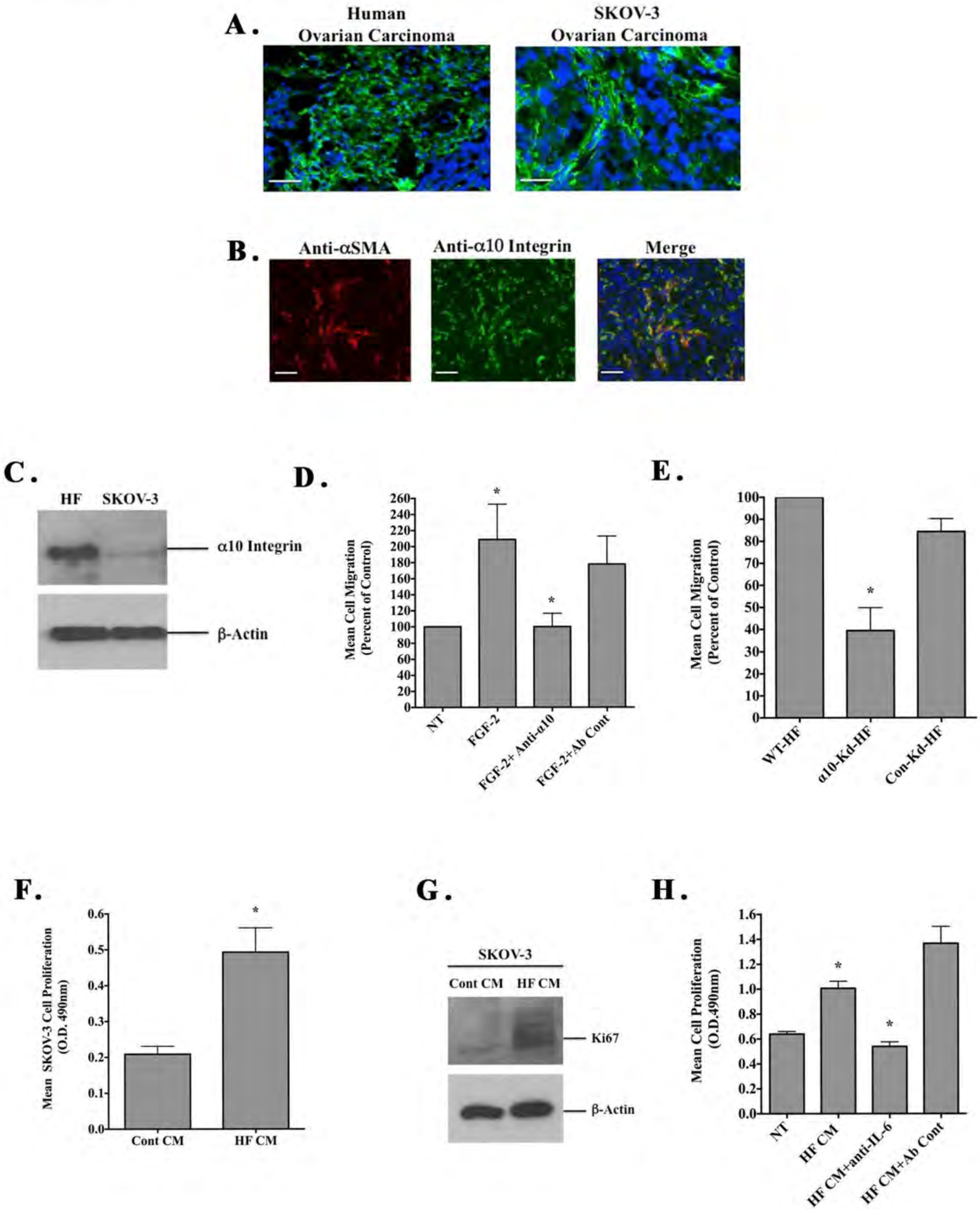
A.
Human
Ovarian Carcinoma
SKOV-3
Ovarian Carcinoma
B.
Anti-αSMA
Anti-α10 Integrin
Merge
C.
HF
SKOV-3
α10 Integrin
β-Actin
D.
Mean Cell Migration
(Percent of Control)
NT
FGF-2
FGF-2+ Anti-α10
FGF-2+Ab Cont
E.
Mean Cell Migration
(Percent of Control)
WT-HF
α10-Kd-HF
Con-Kd-HF
F.
Mean SKOV-3 Cell Proliferation
(O.D. 490nm)
Cont CM
HF CM
G.
SKOV-3
Cont CM
HF CM
Ki67
β-Actin
H.
Mean Cell Proliferation
(O.D.490nm)
NT
HF CM
HF CM+anti-IL-6
HF CM+Ab Cont